A Design of Q-shift Filter for Dual-Tree Complex Wavelet Transforms

Faezeh Yeganli

Submitted to the
Institute of Graduate Studies and Research
in partial fulfillment of the requirements for the Degree of

Master of Science
in
Electrical and Electronic Engineering

Eastern Mediterranean University
January 2010
Gazimagusa, North Cyprus

Approval of the Institute of Graduate Studies and Research

Prof. Dr. Elvan Yilmaz
Director (a)

I certify that this thesis satisfies the requirements as a thesis for the degree of Master of Science in Electrical and Electronic Engineering.

Assoc. Prof. Dr. Aykut Hocanin
Chair, Department of Electrical Engineering

We certify that we have read this thesis and that in our opinion it is fully adequate in scope and quality as a thesis for the degree of Master of Science in Electrical and Electronic Engineering.

Prof. Dr. Runyi Yu
Supervisor

Examining Committee

1. Prof. Dr. Huseyin Ozkaramanli
2. Prof. Dr. Runyi Yu
3. Assoc. Prof. Dr. Hasan Demirel

ABSTRACT

In this work a new method of designing filter for Dual-tree complex wavelet transform is presented. In the new method, the space of orthonormal wavelet filters is defined in terms of some parameters, these parameters are used to design Q-shift filters to have desirable properties including good smoothness and support in [-2p/3, 2p/3]. The constraints in parameterization method lead to wavelets having two vanishing moments. For obtaining the group delay of 1/4 sample period and minimizing the magnitude or energy in stop band [2p/3, p], Kingsbury minimized the energy in this domain. In the proposed method in this work, we minimized the peak magnitude of filters in the stop band. The design approach is illustrated with four examples. The results are compared with Kingsbury's Q-shift in analyticity measures, shift-invariance property and half-sample delay.

The designed filters are then used in image denoising. We used the Bivariate shrinkage algorithm for wavelet coefficient modeling and thresholding. Three images (Boat, Baboon, and Cameraman) have been used for test. The experimental results are compared with those obtained using Kingsbury's Q-shift filters.

Keywords: Dual-tree complex wavelet transforms, Q-shift filters, Orthogonal wavelets, Parameterization, Image denoising.

ÖZ

Bu çalismada Ikili agaç kompleksi dalgacik dönüsümü için filtre tasarlamanin yeni bir yöntemi sunulmaktadir. Yeni yöntemde ortonormal dalgacik filtrelerinin alani parametrelerle belirlenmektedir, sonra bu parametreler iyi pürüzsüzlük ve [-2p/3, 2p/3]'de destek de dahil istenen özelliklere sahip Q-shift filtrelerinin tasarlanmasinda kullanilmaktadir. Parametrizasyon yöntemindeki kisitlar dalgaciklarin iki kaybolma hareketine sahip olmasina neden olmaktadir.

1/4 örnek periyodunun grup gecikmesini elde etmek ve [2p/3, p]'de istenmeyen büyüklük veya enerjiyi asgariye indirmek için Kingsbury bu alandaki enerjiyi minimize etmistir. Bu çalismada önerilen yöntemde filtrelerin tepe büyüklügünü söndürme kusaginda minimize ettik. Sekilli örnekler tasarimin yaklasimini göstermektedir ve sonuçlar çözümleyicilik ölçümündeler, shift-degismezlik özelliginde ve yarim örnek gecikmesinde Kingsbury'nin Q-shift'i ile karsilastirilabilirdir.

Tasarlanan filtreler görüntü gürültüsüzlestirmede kullanilmaktadir. Dalgacik katsayi modellemesi ve esiklemesi için iki degiskenli fire algoritmasini kullandik. Test için üç image (Kayik, Babun ve Kameraman) kullanilmistir ve deneysel sonuçlar Kingsbury'nin Q-shift filtrelerinin kullanilmasiyla elde edilenlerle karsilastirilmistir.

Anahtar sözcükler: Ikili agaç kompleksi dalgacik dönüsümü, Q-shift filtresi, Ortogonal dalgaciklar, Parametrizasyon, Görüntü gürültüsüzlestirme.

To my beloved Father MirMahmoud and Mother Alvan

and

My sweetie sisters Faegheh, Hanieh, and Sepideh

ACKNOWLEDGMENT

I would like to express my sincere thanks to my supervisor Prof. Dr. Runyi Yu for his help and guidance. It was a pleasure and honor for me to work with him.

I owe tremendously a lot to my family who allowed me to travel all the way from Iran to Cyprus and supported me all throughout my studies. I would like to dedicate this thesis to them as an indication of their significance in my life.

I would like to thank H. M Paiva, Empresa Brasileira de Aeronáutica (EMBRAER), São José dos Campos, Brazil, for providing the MATLAB code of parameterization.

Finally, special thanks to my dear friends for their emotional help, encouragements, and supports.

TABLE OF CONTENTS

LIST OF TABLES

LIST OF FIGURES

LIST OF SYMBOLS/ABBREVIATIONS

$c(n)$	Scaling function coefficient
$d(j,n)$	Wavelet coefficient
E_2	Energy of half sample delay error
E_∞	Half-sample delay error
$g_0(n)$	Low pass filter in primal filter bank
$g_1(n)$	High pass filter in dual filter bank
$h_0(n)$	Low pass filter in primal filter banks
$h_1(n)$	High pass filter in dual filter bank
H	Hilbert transform
H_{L2}	4L tap low pass filter
I_2	Analyticity measure
I_∞	Analyticity measure
I_{2H}	Shift invariance measure of primal filter bank
I_{2G}	Shift invariance measure of dual filter bank
$I_{\infty H}$	Shift invariance measure of primal filter bank
$I_{\infty G}$	Shift invariance measure of dual filter bank
c_i	Variable of parameterization method

$f(t)$	Scaling function
$y(t)$	Wavelet
$y_h(t)$	Primal wavelet
$y_g(t)$	Dual wavelet
Bishrinkage	Bivariate shrinkage
CQF	Conjugate quadrature filter
CWT	Complex wavelet transform
DT CWT	Dual tree complex wavelet transform
DWT	Discrete wavelet transform
PDF	Probability distribution function
PSNR	The peak signal to noise ratio
Q-shift	Quarter shift

Chapter 1

INTRODUCTION

1.1 Introduction

Dual-Tree Complex Wavelet Transform (DT CWT) is one of a most important development in signal processing domain. It was first introduced by Kingsbury [1]. Generating complex coefficients by DT CWT introduces limited redundancy and allows the transform to provide shift invariance and directional selectivity of filters. These properties make it useful in areas of signal and image processing [2].

By understanding the concept of Hilbert transform pairs, the DT CWT achieves desirable properties such as nearly shift invariance with limited redundancy. In DT CWT one wavelet is Hilbert transform of the other and scaling filters in primal filter banks should be designed to be offset from each other by a half sample delay [1, 3, 4]. This fundamental concept of Hilbert transform of wavelet bases relates to existence of two filter banks making together a dual-tree of filter banks. If the Hilbert transform pair requirement is satisfied, many properties are shared by the primal and the dual filter bank.

This work is concern with the design of filters for DT CWT structure. There are two approaches to the design of dual-tree filter banks. The first is designing the primal and the dual filter banks at the same time. Kingsbury's Q-shift solution [5] and Selesnick

common factor solution [6] fall in this category. The second is design the dual filter banks from an existing filter banks such as the Daubechies biorthogonal filter bank [5].

The idea of Q-shift filters is presented in the work of Kingsbury in [7, 8] for improving orthogonality and symmetry properties of filter banks in dual-trees. Then a new designed has been proposed in [9] for optimizing the Q-shift filters. In a Q-shift filters a half sample delay is obtained with filter delays of 1/4 or 3/4 of a sample period, and this is achieved with an asymmetric even length primal filter and its time reverse [9].

A parameterization of orthonormal wavelets was introduced by Sherlock and Monro in [10] and recently extended in [11]. The parameterization method enables us to describe the space of orthonormal wavelets in terms of a set of parameters. The coefficients for all orthonormal perfect reconstruction FIR filters are generated with a simple recurrence [10, 11].

In this work, we present a new design technique for Q-shift filters. The new design method is based on parameterization of orthonormal wavelets with two vanishing moments. The peak magnitude of the low pass filter in dual-tree structure is minimized in [2p/3, p] instead of the energy used by Kingsbury. The aim of this work is to design a Q-shift filter according to parameterization of wavelet filters. The proposed approach can lead to an FIR filter bank for analytic complex wavelets. In addition, filter bank properties such as orthogonality, vanishing moments and other properties can be incorporated in the design procedure.

1.2 Organization

The DT CWT is briefly introduced in Chapter 2. Its structure, filter designing and extension to two dimensional are described in this chapter. In Chapter 3, a Q-shift filter design is defined and filter requirements for Q-shift filter design are explained. Then the parameterization method is introduced. We present design examples in this chapter. After designing, the mathematical properties of designed filter related to its analyticity and shift invariance are considered and compared with Kingsbury's Q-shift filters.

In Chapter 4, we study the application of DT CWT in image denoising. Several standard images are used to study the denoising problem. Each image is corrupted by an additive white Gaussian noise at various levels and then denoised by using a DT CWT. The denoising method is used for three images (Boat, Baboon and Cameraman). The results of denoising are illustrated in this chapter.

Chapter 5 summarized the material presented in this work. It also discusses the possible future work.

Chapter 2

DUAL-TREE COMPLEX WAVELET TRANSFORM

2.1 Introduction

A Dual-Tree Complex wavelet Transform (DT CWT) is a recently development in wavelet domain that was first produced by Kingsbury in [1]. Its structure with good properties likes shift-invariance and good directionality in two and higher dimensions make it useful in signal and image processing applications. It achieves this with a limited redundancy (redundancy factor of 2^D for D dimensional signals).

In this chapter we will introduce DT CWT. At first we briefly explain wavelet domain analysis, and then Discrete Wavelet Transform (DWT) and its properties. Then DT CWT and its characterization are introduced and filter designed procedure for DT CWT is explained. Finally we explain extension of the DT CWT to two dimensional (2D).

2.2 Wavelet Transform

Wavelets are famous domain in signal processing. They are stretched and shifted version of real valued band pass wavelets $y(t)$. Their combination with low pass scaling function $f(t)$ can form an orthonormal basis expansion that provides a time-frequency

analysis of signal. We can express any signal $x(t)$ in terms of wavelets and scaling function as in (2.1) [2]:

$$x(t) = \sum_{n=-\infty}^{\infty} c(n)f(t-n) + \sum_{j=0}^{\infty}\sum_{n=-\infty}^{\infty} d(j,n)2^{j/2}y(2^j t - n) \tag{2.1}$$

where $c(n)$ is the scaling function coefficient, and $d(j,n)$ is the wavelet coefficient that are computed respectively:

$$c(n) = \int_{-\infty}^{\infty} x(t)f(t-n)dt \tag{2.2}$$

$$d(j,n) = 2^{j/2}\int_{-\infty}^{\infty} x(t)y(2^j t - n)\ . \tag{2.3}$$

Time-frequency analysis is controlled by scale factor j and time factor n.

There are algorithms to compute a scaling function and wavelet based on weighted sum of shifted scaling function (basis) that produce a discrete-time low pass filter $h_0(n)$ and high pass filter $h_1(n)$, and upsampling and downsampling operations which make filter banks structure. The DWT consists of recursively applying two-channel filter bank shown in Figure 2.1. We refer to [2, 12] on theory about wavelet domain analysis.

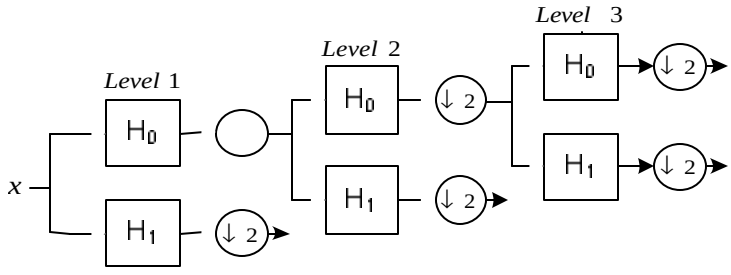

Filters $h_0(n)$, $h_1(n)$ makes a convenient parameterization for designing wavelets and scaling functions with properties like compact support, orthogonality to lower order polynomials (vanishing moments). These properties make wavelets more useful than Fourier analysis, and enable to represent many types of signals which are not matched by the Fourier basis [2].

The DWT have these properties: good compression of signal energy, perfect reconstruction with short support filters, no redundancy and very low computation. In spite of good properties with real wavelets, there are some fundamental problems [4]:

1) Oscillations: Wavelets are band pass functions, so their coefficients oscillate positive and negative around singularities (jump and spikes); this makes wavelet based processing to have some complexities.
2) Shift variance: The wavelet coefficients will oscillate around singularities by a small shift of signal, though it complicates wavelet domain processing.
3) Aliasing: Computing wavelet coefficients by discrete time upsampling and down sampling operations makes aliasing.
4) Lack of directionality: Multi dimensional wavelet coefficients produce a pattern that is simultaneously oriented in several directions. This lack of directional selectivity makes problems in image processing.

Complex wavelets provide solution to these shortcomings [2].

2.3 Complex Wavelets and DT CWT

The DWT's problems [2] solved by Fourier transform's properties. Unlike the DWT, Fourier transform doesn't suffer from mentioned problems. The Fourier transform analysis is based on complex complex-valued oscillating sinusoids:

$$e^{j\Omega t} = \cos(\Omega t) + j\sin(\Omega t). \tag{2.4}$$

The oscillating real part (cosine) and imaginary part (sine) components form a Hilbert transform pair that produce an analytic signal $e^{j\Omega t}$ which is supported on only half of the frequency axis ($\Omega > 0$).

Imitating the above representation, we can get a Complex wavelet transform (CWT) with complex valued scaling function [2]:

$$y_C(t) = y_r(t) + jy_i(t). \tag{2.5}$$

A complex valued wavelet coefficient is defined as below:

$$d_C(j,n) = d_r(j,n) + jd_i(j,n). \tag{2.6}$$

According to (2.4) and (2.5), $y_r(t)$ is real and even and $y_i(t)$ is imaginary and odd and by forming the Hilbert transform pair they make $y_C(t)$ to be analytic signal [2]. These properties are illustrated in Figure 2.2.

The design of CWT makes some new problems that DWT doesn't have, so new approach is needed.

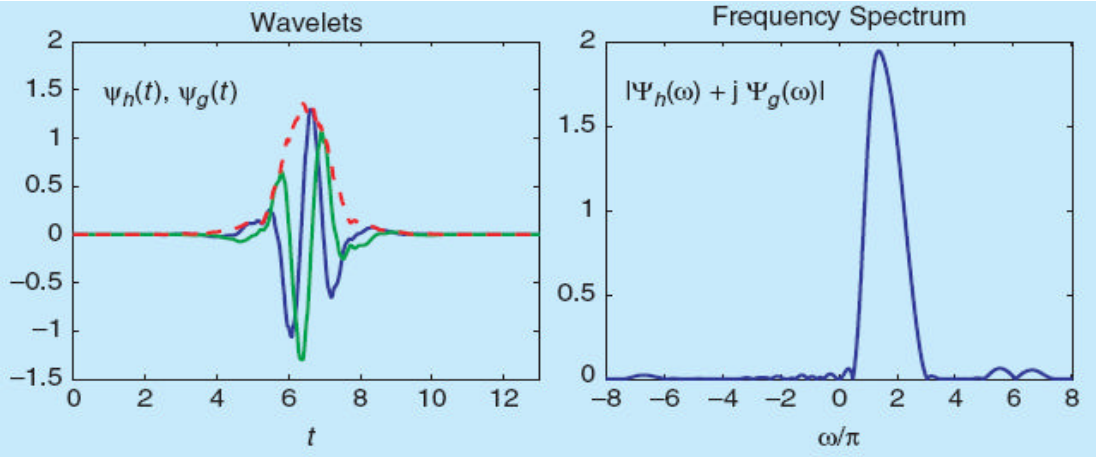

Figure 2.2: Complex wavelets with analyticity property [2]

2.3.1 The DT CWT

For implementing an analytic wavelet transform, Kingsbury introduced a DT CWT structure in [1]. The DT CWT employs two real DWT in its structure. The first DWT gives the real part of the transform and second part gives the imaginary part. The analysis and synthesis Filter banks used in DT CWT are shown in Figures 2.3 and 2.4 respectively.

The two real wavelet transforms use two different set of filters that satisfying the perfect reconstruction condition. Filters $h_0(n)$, $h_1(n)$ and $g_0(n)$, $g_1(n)$ denote the low pass/high pass filter pairs for the upper and lower filter banks respectively. Both filters are real but their combination produce a complex wavelet. For satisfying a perfect reconstruction condition the filters are designed to make a complex wavelet $y(t) = y_h(t) + jy_g(t)$ approximately analytic by two real wavelet transforms $y_h(t)$ and $y_g(t)$. Equivalently they are designed so that the lower wavelet $y_g(t)$ is the Hilbert transform of upper wavelets $y_h(t)$; $y_g(t) \approx \mathrm{H}\{y_h(t)\}$ [2, 3, 6].

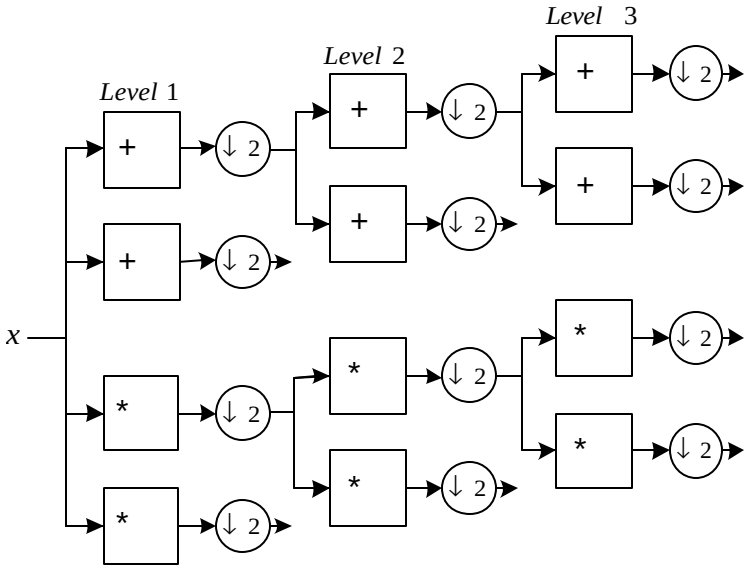

Figure 2.3: Analysis filter banks of DT CWT

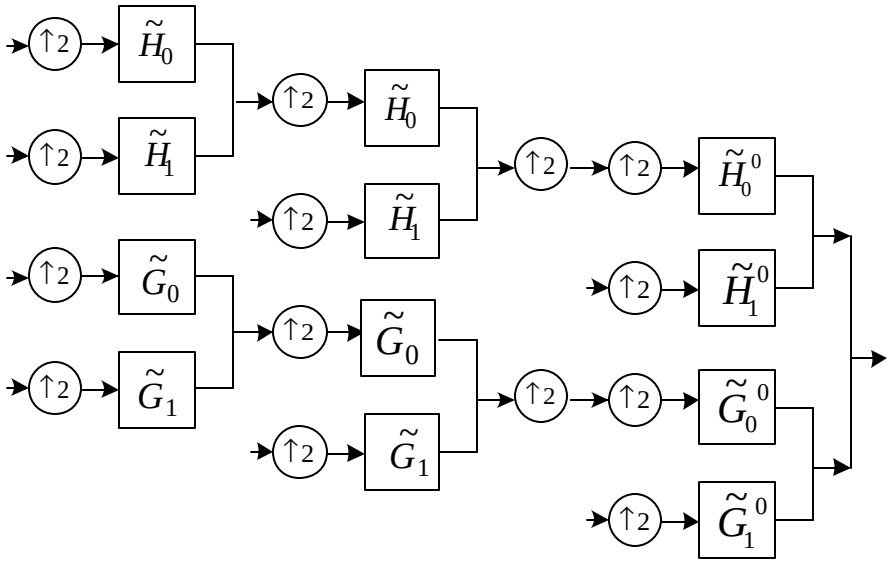

Figure 2.4: Synthesis filter banks of DT CWT

In the inverse of DT CWT, like the forward transform, the real part and imaginary part are each inverted and the inverse of the two real DWTs gives a two real signal and finally the average of two real signals gives a final output. We can get an original signal from either real part or imaginary part alone.

2.3.2 The Half Sample Delay Condition

Several analysis are made about the fact that one wavelet is approximately the Hilbert transform of the other. If we want wavelets form a Hilbert transform pair, we need to design low pass filters satisfying this property. Now let

$$y_h(t) = \sqrt{2}\sum_n h_1(n) f_h(t) \tag{2.7}$$

$$f_h(t) = \sqrt{2}\sum_n h_0(n) f_h(t) \tag{2.8}$$

where $h_1(n) = (-1)^n h_0(d-n)$; for lower filter bank $y_g(t)$, $f_g(t)$ and $g_1(n)$ are defined similarly. Assuming that both real wavelets are orthonormal, from [2, 3] these filters should satisfy the property as below:

$$g_0(n) \approx h_0(n-0.5)\ . \tag{2.9}$$

It means that one of them should be approximately half sample shift of the other. The Fourier transform of (2.9) and its magnitude and phase are

$$G_0(e^{jw}) = e^{-j0.5w} H_0(e^{jw}) \tag{2.10}$$

$$\left|G_0(e^{jw})\right| = \left|H_0(e^{jw})\right| \tag{2.11}$$

$$\angle G_0(e^{jw}) = \angle H_0(e^{jw}) - 0.5w\ . \tag{2.12}$$

By having this property, wavelets will form Hilbert transform pair ($y_g(t) \approx \mathrm{H}\{y_h(t)\}$) and the complex wavelet $y_h(t) + jy_g(t)$ will be approximately analytic, and the DT DWT is nearly shift-invariant. Also when the complex wavelets are analytic, the two filter banks share common properties including orthogonality (or biorthogonality) [13, 14].

Now we understand the aim of the Hilbert transform of wavelet bases. This fundamental concept relates to the existence of two filter banks making together a dual-tree of filter banks.

2.4 Filter Design for the DT CWT

As mentioned in the previous sections, filter properties in the filter banks structure play a significant role in obtaining the important properties of wavelet domain. So designing filters that satisfy these properties is important.

Several methods proposed for designing filters for the DT CWT structure. In these methods the designed filters have some desired properties like: approximately half-sample delay property, perfect reconstruction, finite support filters (FIR filters), vanishing moments, linear phase filters.

The early methods for designing filters include linear-phase biorthogonal solution, Q-shift solution, and common factor solution. The first method is introduced in [1, 16]; common factor solution is explained in [6]; and Q-shift method that we used for designing a filter in this thesis is introduced by Kingsbury in [7]; and will be explained in next section. See [2] and [13] for more about the design of DT filter banks.

The other important thing in filter designing for dual-trees is that the first stage of the dual-tree filter banks should be different from the other stages. The half sample delay condition shouldn't be used for the first stage. For the first stage, it is necessary only to translate one set of filters by one sample to the other ($g_0(n) = h_0(n-1)$) and any set of perfect reconstruction filter can be used for first stage. For more explanation and its proof we refer to [2].

2.4.1 Q-shift Filter Design

This method was introduced by Kingsbury in [7]. Satisfying linear-phase property of $h_0(n)$ is achieved by

$$g_0(n) = h_0(N-1-n) \ . \tag{2.13}$$

where N (even) is the length of $h_0(n)$ which is supported in $0 \le n \le N-1$. In this case the magnitude part of (1.12) is satisfied but the phase part (2.12) is not and will be like below [2]:

$$\left|G_0(e^{jw})\right| = \left|H_0(e^{jw})\right| \tag{2.14}$$

$$\angle G_0(e^{jw}) \neq \angle H_0(e^{jw}) - 0.5w \ . \tag{2.15}$$

The quarter-shift solved (2.15) problem. From (2.13) we can write

$$G_0(e^{jw}) = \overline{H_0(e^{jw})} e^{-j(N-1)w} \ . \tag{2.16}$$

And its phase becomes

$$\angle G_0(e^{jw}) = -\angle H_0(e^{jw}) - (N-1)w \ . \tag{2.17}$$

From (2.12) we can rewrite (2.17) like below:

$$\angle H_0(e^{jw}) - 0.5w \approx -\angle H_0(e^{jw}) - (N-1)w . \tag{2.18}$$

Then we can obtain below formula:

$$\angle H_0(e^{jw}) \approx -0.5(N-1)w + 0.25w . \tag{2.19}$$

So, $h_0(n)$ is approximately linear-phase and symmetric around $n = 0.5(N-1) - 0.25$; that is a quarter away from a natural point of symmetry. So this method is named Q-shift method. In Q-shift method the imaginary part of the complex wavelet is a time-reversed of real part ($y_g(t) = y_h(N-1-t)$) [2, 7].

Therefore Q-shift method is to design filters satisfying perfect reconstruction condition and approximately linear-phase condition with group delay required to be a quarter.

2.5 Two-Dimensional DT CWT

One of the advantages of DT CWT is that it can be used to implement two-Dimensional (2D). In 2D, DT CWT saved desirable properties of 1D case and has effective properties like directional selectivity. In particular, 2-D dual-tree wavelets are not only approximately analytic but also oriented and thus natural for analyzing and processing oriented singularities like edges in images [2].

At first we explains 2D DWT and then discuss 2D DT CWT. Using the wavelet transform for image processing requires implementation of a 2D version of analysis and synthesis filter banks. In this case, first, 1D analysis filter banks is applied to the columns of the image and then applied to the rows. Therefore four sub-band images (LL, LH, HL, HH) are obtained; see Figure 2.5. For obtaining original image, the 2D synthesis filter bank combines the four sub-band image [2].

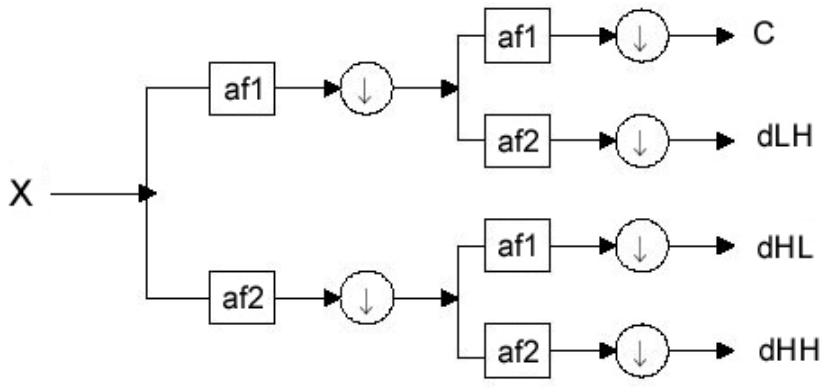

Figure 2.5: Wavelet decomposition of an image in one stage [21]

The separable (row-column) implementation of the 2D DWT is characterized by three wavelets as below [2]:

$$y_1(x,y) = f(x)y(y) \quad \text{(LH wavelet)}$$

$$y_2(x,y) = y(x)f(y) \quad \text{(HL wavelet)}$$

$$y_3(x,y) = y(x)y(y) \quad \text{(HH wavelet)}.$$

The LH (Low-High) and HL wavelets are oriented vertically and horizontally, the HH wavelets mix two diagonal orientations ($+45^\circ$ and -45°). Figure 2.6 illustrates these wavelets [21].

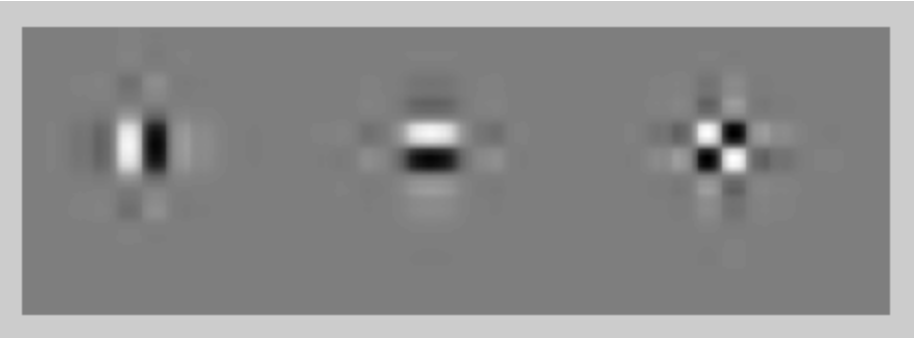

Figure 2.6: The wavelets in space domain (LH, HL, and HH) [21]

The separable DWT is unable to isolate these orientations. 2D DT CWT produce oriented wavelets that are oriented in six distinct directions. In each direction, one of the two wavelets can be interpreted as the real part while the other wavelet can be interpreted as the imaginary part of the complex-valued 2D wavelet. The complex 2D DT operating as four critically sampled separable 2D DWTs operating in parallel. The Figure 2.7 illustrates 2D DT CWT.

We can see in Figure 2.7, the wavelets are oriented in the same six directions but there are two in each direction. The six wavelets on the first are interpreted as a real part

and the six wavelets on the second row are imaginary part of a set of six complex wavelets. The third row is the magnitude of the six complex wavelets [21].

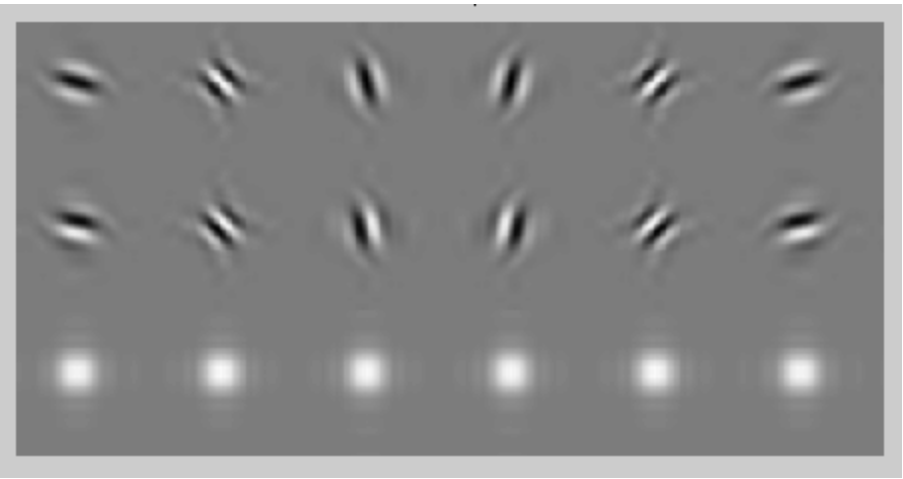

Figure 2.7: 2D dual-tree complex wavelets [21]

While the wavelets are oriented, approximately analytic, and non-separable, the implementation is very efficient and makes it useful in many applications of image processing such as denoising.

Chapter 3

Q-SHIFT FILTER DESIGN OF DUAL-TREE FILTER BANKS

3.1 Introduction

We have described the DT CWT. This introduces limit redundancy and allows the transform to provide approximate shift invariance and directionality selection of filters while preserving the usual properties of perfect reconstruction and computational efficiency responses. We analyze the new designed filters in terms of directionality and shift invariance.

In this chapter we present a new design of Q-shift filters for DT CWT. The idea of using Q-shift approach is motivated by the work of Kingsbury in [7] for improving orthogonality and symmetry properties of filter banks. Q-shift form employs a single design of even-length filter with asymmetric coefficients. The DT CWT structure requires most of the wavelet filters to have a well controlled group delay [7, 9] (equivalent to quarter of a sample period) to achieve approximately shift invariance.

In Q-shift filters a half-sample delay difference is obtained with filter delays of 1/4 and 3/4 of a sample period and this is achieved with an asymmetric even-length filter $H_0(z)$ and its time reverse. Also lower tree filters are time-reverse of upper tree filters and reconstruction filters are the time-reverse of analysis filters, this make transform use

shorter filters and all filters form orthonormal set (bases are orthonormal) beyond level one. Then the two trees are matched very well and have a more symmetric sub-sampling structure [7, 15].

In this work we use parameterization method of orthogonal wavelet filter banks. This method was first introduced by Sherlock and Monro in [10] and then extended in [11]. According to the mentioned method, the space of orthonormal wavelet is described by a set of parameters [10]. The parameterization is not unique for different roots of the polynomial may be chosen. The advantage of this method is that it is able to parameterize wavelets that have vanishing moments greater than one, in this work is equal to two [11].

As we know one of the most important properties of complex wavelet filters in dual-tree filter banks is their analyticity. Other important mathematical properties of complex wavelet filters are consequences of analyticity.

In Section 3.2, the requirements of Q-shift filter design will explain. In Section 3.3 the parameterization method will introduced. The design procedure is given in Section 3.4; Section 3.5 presents some design examples. The mathematical properties of complex wavelet filters introduced and their comparison between designed Q-shift filter and Kingsbury's Q-shift filter are shown in Section 3.6.

3.2 Filter Requirements for Q-shift Complex Wavelets

Consider the Q-shift dual-tree in Figure 3.1 in which all filters beyond level 1 are even-length.

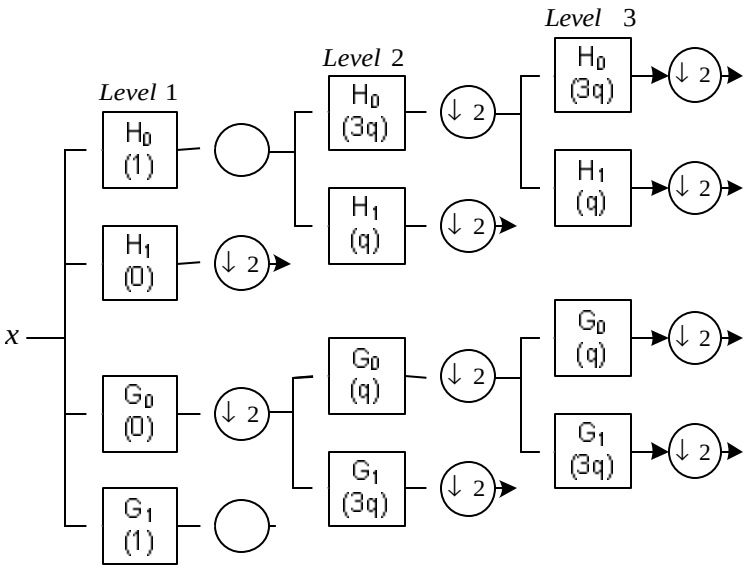
Level 1
Level 2
Level 3
x
H0 (1)
H1 (0)
G0 (0)
G1 (1)
H0 (3q)
H1 (q)
G0 (q)
G1 (3q)
H0 (3q)
H1 (q)
G0 (q)
G1 (3q)
↓ 2

$$G_0(z) = H_0(z^{-1}) \ . \tag{3.4}$$

4) Group Delay ≈ 1/4 sample for H_0 and 3/4 for G_0: To get this property we use Kingsbury's method in [7, 9]. To obtain 2L-tap low pass filters, H_0 and G_0 with 1/4 and 3/4 sample delays, a 4L-tap linear phase and symmetric low pass filter $H_{L2}(z)$ with a delay of 1/2 sample is designed as follows

$$H_{L2}(z) = H_0(z^2) + z^{-1}H_0(z^{-2}) \ . \tag{3.5}$$

So the subsample filter H_0 will have a half of delay of $H_{L2}(z)$ (1/4 sample).

5) Good smoothness when iterated over scale.

6) Finite support in (-2p/3, 2p/3), that is, $H_0(e^{jw}) \approx 0$ For $w \notin$ [-2p/3, 2p/3].

To achieve the fifth and sixth properties we come back to one of the important properties of discrete-time systems that are shift invariant. We say, a discrete-time system is μ-shift-invariant if a shift in input results the output shifted as well [16]. And the M-fold decimator (down sampler) is μ-shift-invariant for input if its frequency supports in not more than 2p/M and the output shouldn't have the aliasing term in same frequency band with length of $2p$. As we know one of the most important properties of DT CWT structures is its shift invariance property and for achieving this property the conjugate quadrature filters (CQF) should have support limited in [-2p/3, 2p/3], in addition to the well known half sample delay condition at high levels and the one sample delay condition in first level [16].

Analyticity of the complex wavelet filters alone is not enough for the μ-shift-invariant of DT CWT. We should know that the stop band of $H_0(z)$ at each

scale suppresses energy at frequencies where unwanted pass bands appear from sub sampled filters operating at coarser scales [9, 16]. So we should minimize the magnitude spectrum or energy in [2p/3, p]. This cut off frequency has been used by Kingsbury for designing his Q-shift filter. This analysis of µ-shift-invariant helps explain the success of Q-shift filters in DT CWT based applications.

In this work for obtaining the group delay of 1/4 sample period and minimizing the magnitude of the $H_0(z)$ in the mentioned method we use $H_{L2}(z)$ as in [7, 9] and minimize the maximal magnitude of $H_{L2}(z)$ instead of the energy used in Kingsbury's design in its stop band of [p/3, p].

Minimizing the magnitude of $H_{L2}(z)$ in the mentioned domain and finally obtain the Q-shift filter are explained in next section.

7) Vanishing moments: Vanishing moments are feature of wavelets. They are the number of zeros of scaling filter at $z = -1$. Having P vanishing moments means that wavelets coefficients for Pth order polynomial will be zero. That is any polynomial signal up to P-1 can be represented completely in scaling space. More vanishing moments means that scaling function can represent more complex signals accurately. In this work our design procedure let us to have two vanishing moments.

3.3 A Parameterization of Orthonormal Filters

The parameterization of the space of two-channel orthonormal FIR filters enable us to describe the generation of all filters by using a simple recurrence. The method used here for wavelets has guaranteed the resulting wavelets have two vanishing moments.

The remaining degrees of freedom are re-parameterized which lead to a convex set of feasible parameter values [11].

Let $H_0(z)$ be 2L (= N) length low pass filter, Sherlock and Monro's recursive formulas for a filter of length 2(L+1) according to terms of 2L length filter, expressing the coefficients as in [11]

$$\begin{cases} h_0^{(1)} = \cos(a_1) \\ h_1^{(1)} = \sin(a_1) \end{cases} \tag{3.6}$$

$$\begin{cases} h_0^{(L+1)} = \cos(a_{L+1}) h_0^{(L)} \\ h_{2i}^{(L+1)} = \cos(a_{L+1}) h_{2i}^{(L)} - \sin(a_{L+1}) L_{2i-1}^{(L)}, \ i = 1,2,..., L-1 \\ h_{2L}^{(L+1)} = -\sin(a_{L+1}) h_{2L-1}^{(L)} \end{cases} \tag{3.7}$$

$$\begin{cases} h_1^{(L+1)} = \sin(a_{L+1}) h_0^{(L)} \\ h_{2i+1}^{(L+1)} = \sin(a_{L+1}) h_{2i}^{(L)} + \cos(a_{L+1}) h_{2i-1}^{(L)}, \ i = 1,2,..., L-1 \\ h_{2L+1}^{(L+1)} = \cos(a_{L+1}) h_{2L-1}^{(L)}. \end{cases} \tag{3.8}$$

As we see that the orthonormal wavelet filters can be completely parameterized by L angles $a_i, 1 \le i \le L$, which can assume any value in the set of real numbers and any choice of a_i will lead to a valid orthonormal FIR filter banks system, and any system can be expressed in terms of some choice of a_i [10, 11].

For a first vanishing moment the following condition should be satisfied

$$H_0(z)\big|_{z=-1} = 0 \ . \tag{3.9}$$

From (3.7)-(3.9) we can write $H_0^{(L)}(z)$ with angles a_i as below

$$H_0^{(L)}\big|_{z=-1} = \cos \sum_{i=1}^{L} a_i - \sin \sum_{i=1}^{L} a_i \ . \tag{3.10}$$

So the first vanishing moment condition will become:

$$a_L = \frac{p}{4} - \sum_{i=1}^{L-1} a_i \ . \tag{3.11}$$

For second vanishing moment it is necessary to impose this condition:

$$\frac{dH_0^{(L)}(z)}{dz}\Big|_{z=-1} = 0 \ . \tag{3.12}$$

And finally by doing some mathematical expressions on (3.12) and using above formulas the second vanishing moment condition will be obtained (The expression and proof are in [11]):

$$a_{L-1} = \frac{1}{2}\arcsin\left\{-\frac{1}{2} - \sum_{k=1}^{L-2}[\sin \sum_{i=1}^{k} 2a_i]\right\} - \sum_{k=1}^{L-2} a_k \ . \tag{3.13}$$

Vanishing moments conditions reduces the number of free parameters to L-1 and L-2 respectively. For defining a convex region of parameters in R^{L-2} a new parameter c is proposed [11]. Second vanishing moment condition (formula (3.13)) have a real-valued solution, if and only if the angles a_i, $1 \le i \le L-2$, satisfy the following constraints:

$$-\frac{3}{2} \le \sum_{k=1}^{L-2}(\sin \sum_{i=1}^{k} 2a_i) \le \frac{1}{2} \ . \tag{3.14}$$

But these constraints don't define a convex region in R^{L-2}, so for having a convex region c is defined as:

$$c_k = \sin \sum_{k=1}^{k} 2a_i \ , \ 1 \le k \le L-2 \ . \tag{3.15}$$

The constraints can be rewritten as:

$$-\frac{3}{2} \le \sum_{k=1}^{L-2} c_k \le \frac{1}{2} \tag{3.16}$$

$$-1 \le c_1, c_2, ..., c_{L-2} \le 1 \ . \tag{3.17}$$

And the values of $a_i, 1 \le i \le L-2$ are obtained by using the following equations:

$$a_1 = \frac{1}{2}\arcsin(c_1) \tag{3.18}$$

$$a_i = \frac{1}{2}\arcsin(c_i) - \sum_{k=1}^{i-1} 2a_k \ . \tag{3.19}$$

Finally the filter banks coefficients are calculated by (3.6)-(3.8).

By using this method of parameterization in our work we can design Q-shift filer with mentioned properties. The design procedure is explained in next section.

3.4 Q-shift Filter Design Procedure

Following discussions in Sections 3.2 and 3.3, we now give a design procedure for Q-shift filter. By knowing the properties of filter; the design procedure starts with specifying the value of c_i. Parameter c_i is very important parameter in our designing and produces a convex region for our parameterization. After parameterization, the magnitude of obtained filter according to the parameters is minimized and finally the favorite filter will be obtained by recurrence formula. In the following we explain the design procedure step by step.

Step 0. Specify the basic properties of filter like length of scaling filter.

Step 1. Initialize the value of c_i, then generate the a_i by using (3.18) and (3.19).

Step 2. Obtain h_0 from a_i. At first get a_L from (3.11) and (3.13), then h_0 is obtained from (3-6)-(3.8).

Step 3. Define the H_{L2} as in (3.5). Then define the magnitude of $H_{L2}(z)$ in [p/3, p]. This is for obtaining H_0 and G_0 with 1/4 and 3/4 sample period respectively.

Step 4. Minimize the peak magnitude of $H_{L2}(z)$. This is for achieving properties 6 and 7 (Section 3.2) to obtain optimal magnitude.

For minimizing the magnitude of H_{L2} we use constrained minimization method by employing ''fmincon'' in the optimization toolbox of MATLAB. This function can find a constrained minimum of a function with several variables. Our variable here is c and according to the constraints that we defined for c to obtaining the convex region of parameterization, it can start to minimize the magnitude of H_{L2}.

Step 5. Obtain the low pass filter h_0 using ?. Then obtain g_0 from h_0, according to relationship of dual-tree filters in Q-shift filter ($G_0(z) = H_0(z^{-1})$).

The procedure can be repeated with obtained ? as initial value in Step 1. After designing the filters, the complex wavelet $y_h + jy_g$ is expected to be approximately analytic.

3.5 Design Examples

We present four examples in this section to illustrate the design approach and its results. Design examples give filters of length 12, 14, 16, and 18 respectively. The normalized coefficients of h_0 for the mentioned lengths are shown in table 3.1. As we mentioned in previous section we can easily get the g_0 (dual filter bank) by flipping h_0.

Table 3.1: Coefficients of Q-shift filter h_0

N= 12	N= 14	N= 16	N= 18
0.00017654	-0.00754976	-0.00246667	0.00000682
0.00202905	-0.00440359	-0.00070423	0.00003496
0.01944400	0.00135387	0.01485766	0.00006221
-0.05470174	0.00796048	0.00489657	0.00343113
-0.02152764	-0.08771886	0.03152301	-0.01604502
0.40680833	0.03250019	-0.07051195	0.01037313
0.55064137	0.42397196	-0.03670630	-0.04315593
0.15754572	0.50635403	0.42121140	-0.02872404
-0.05006905	0.19977468	0.52959241	0.40720354
-0.01156524	-0.10585055	0.17913806	0.55129394
0.00133476	-0.02542829	-0.04230220	0.15565237
-0.00011613	0.05588967	-0.01602463	-0.05172803
	-0.00440359	0.00589103	-0.00687361
	0.00754976	-0.01936757	0.01534684
		-0.00038895	0.00311584
		0.00136235	-0.00002133
			0.00003377
			-0.00000659

Figures 3.2, 3.6, 3.10 and 3.14 show the normalized coefficients of h_0. For different lengths the magnitude and phase response of h_0 are illustrated in Figures 3.3, 3.7, 3.11, and 3.15. The group delay of h_0 are shown in Figures 3.4, 3.8, 3.12, and 3.16. Finally the analytic wavelet $y_h + jy_g$ for mentioned lengths are depicted in Figures 3.5, 3.9, 3.13, and 3.17.

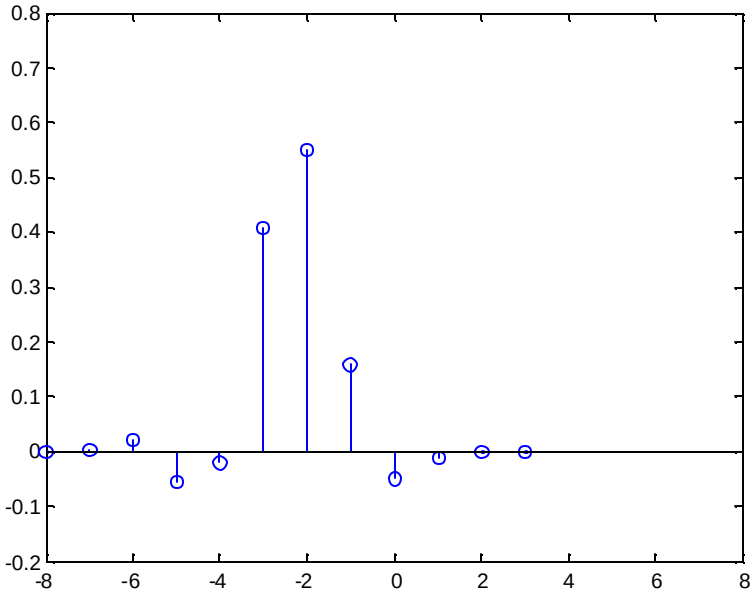

Figure 3.2: Normalized coefficients of h_0 (length= 12)

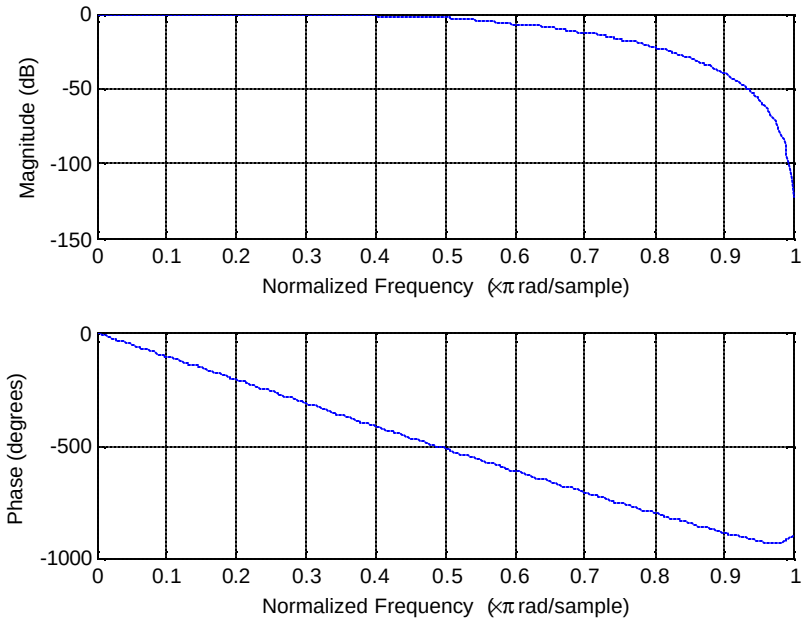

Figure 3.3: Magnitude and phase response of h_0 (length= 12)

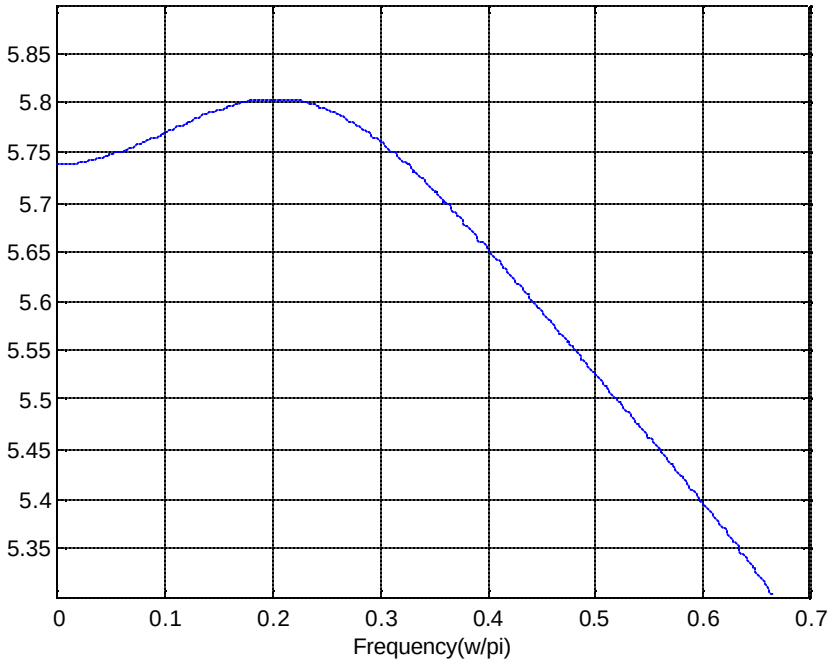

Figure 3.4: Group delay of scaling filter h_0 (length=12)

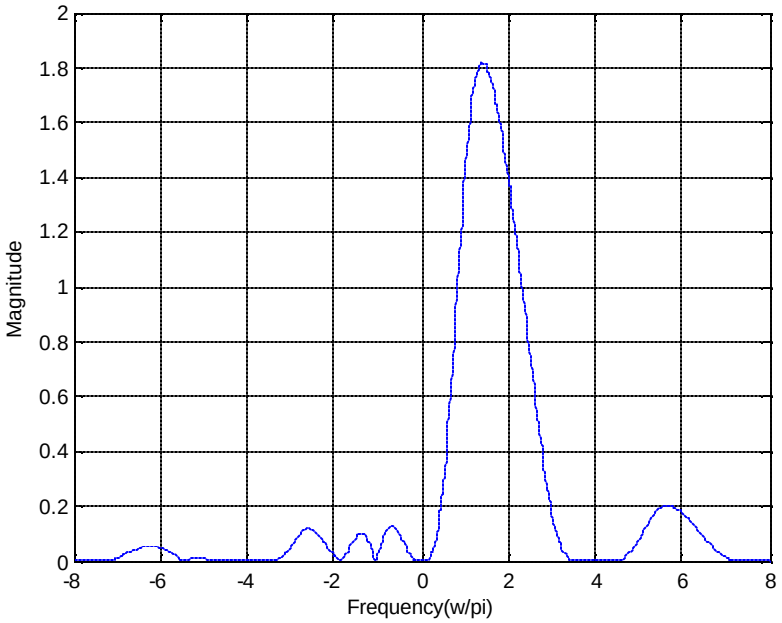

Figure 3.5: Magnitude spectra of complex wavelets $y_h + jy_g$ (length= 12)

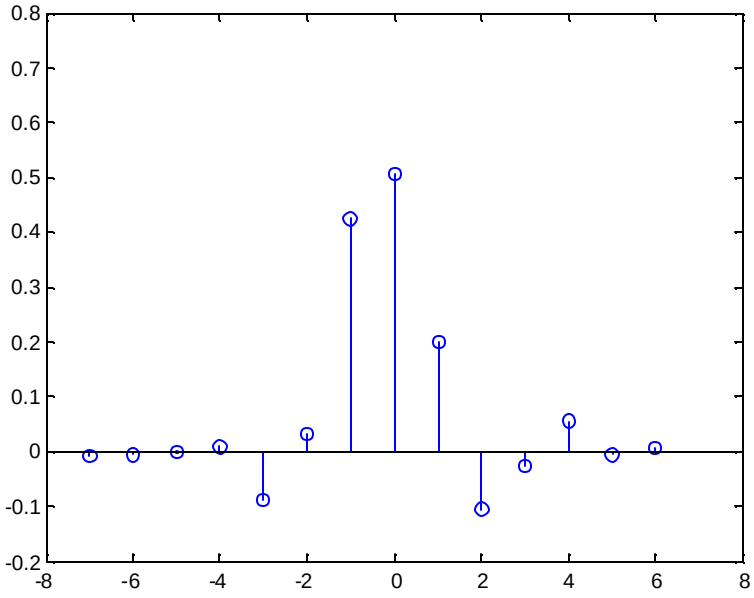

Figure 3.6: Normalized coefficients of h_0 (length= 14)

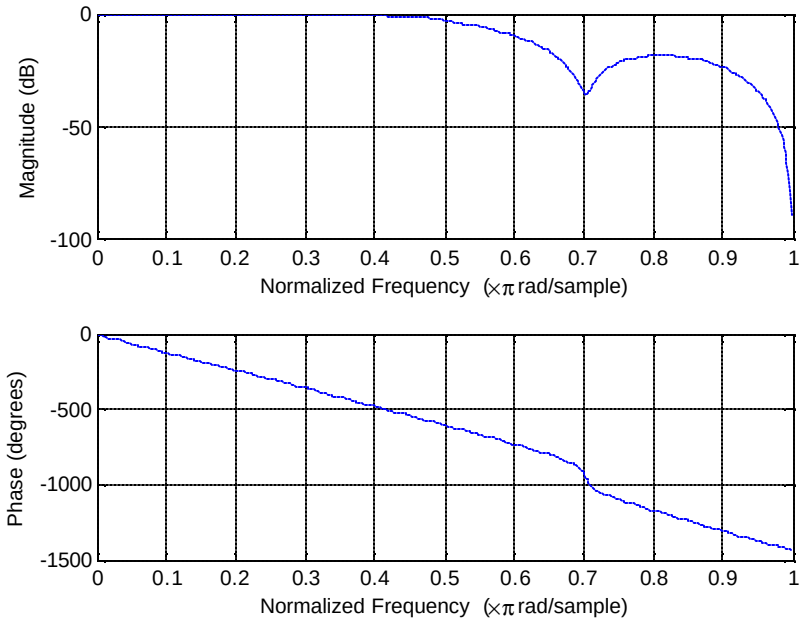

Figure 3.7: Magnitude and phase response of h_0 (length=14)

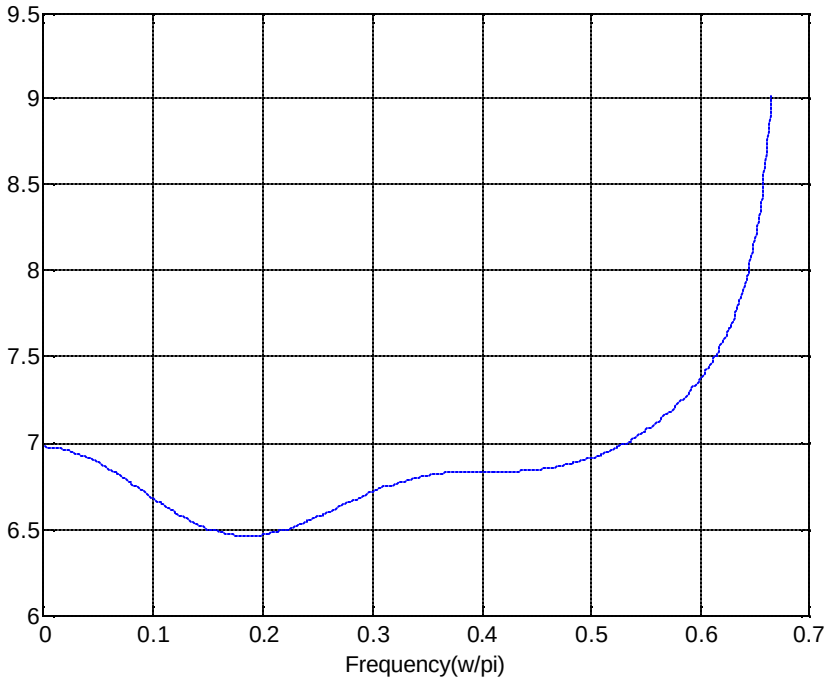

Figure 3.8: Group delay of scaling filter h_0 (length= 14)

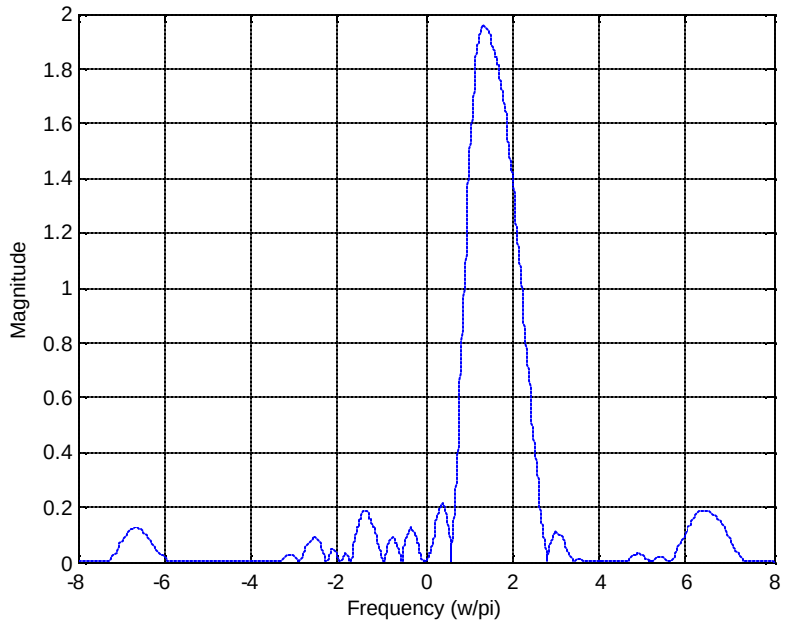

Figure 3.9: Magnitude spectra of complex wavelets $y_h + jy_g$ (length= 14)

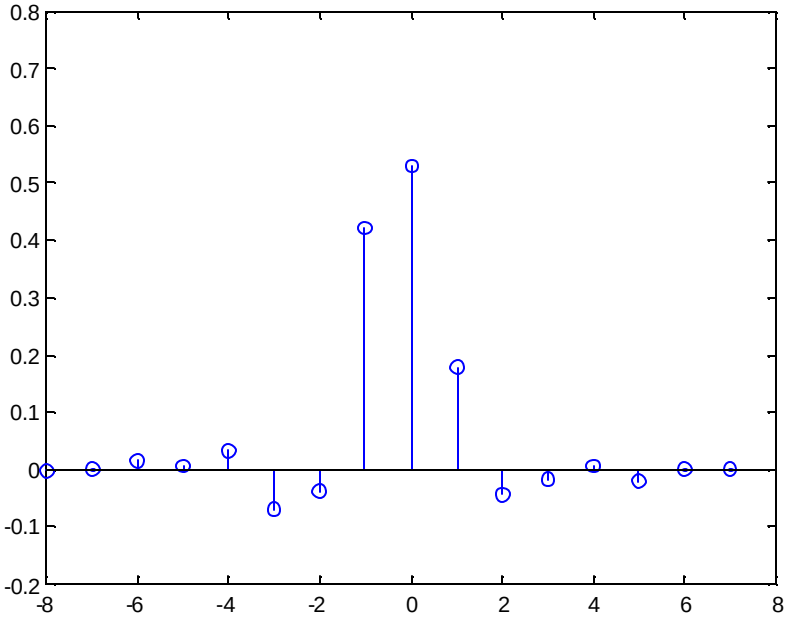

Figure 3.10: Normalized coefficients of h_0 (length= 16)

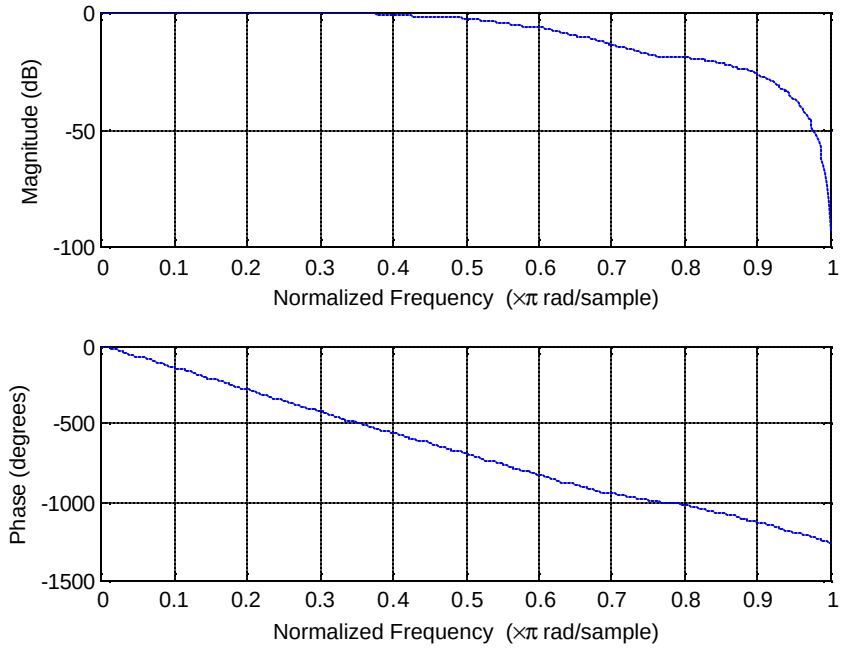

Figure 3.11: Magnitude and phase response of h_0 (length= 16)

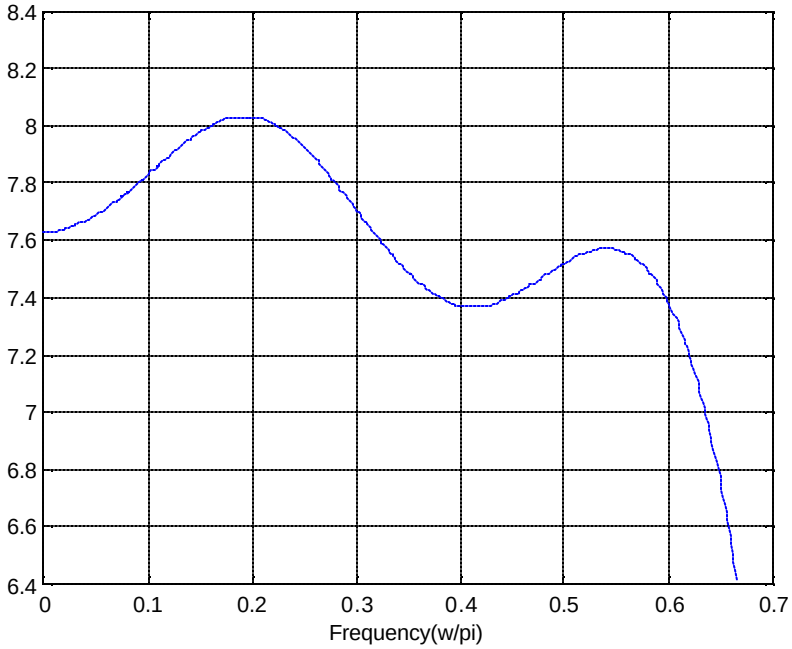

Figure 3. 12: Group delay of scaling filter h_0 (length= 16)

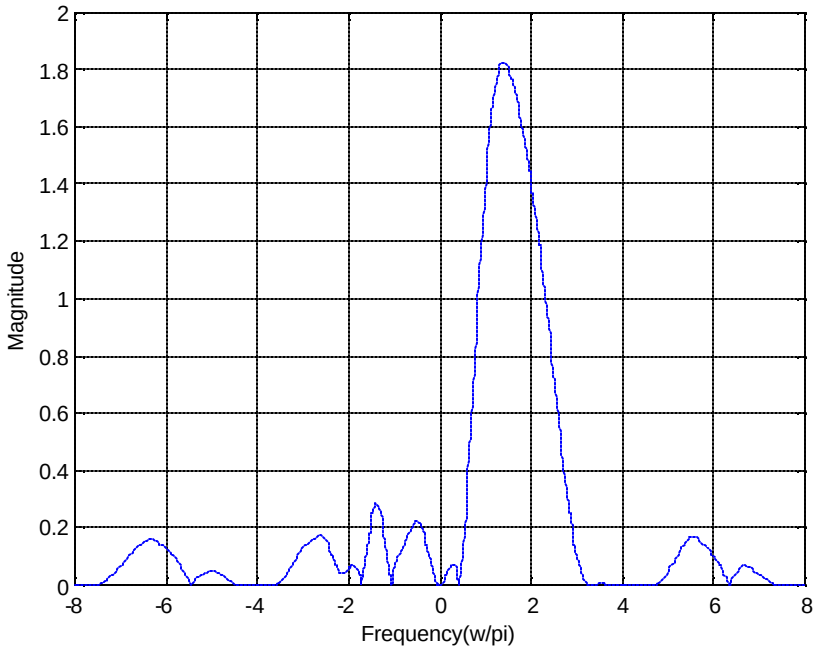

Figure 3.13: Magnitude spectra of complex wavelets $y_h + jy_g$ (length= 16)

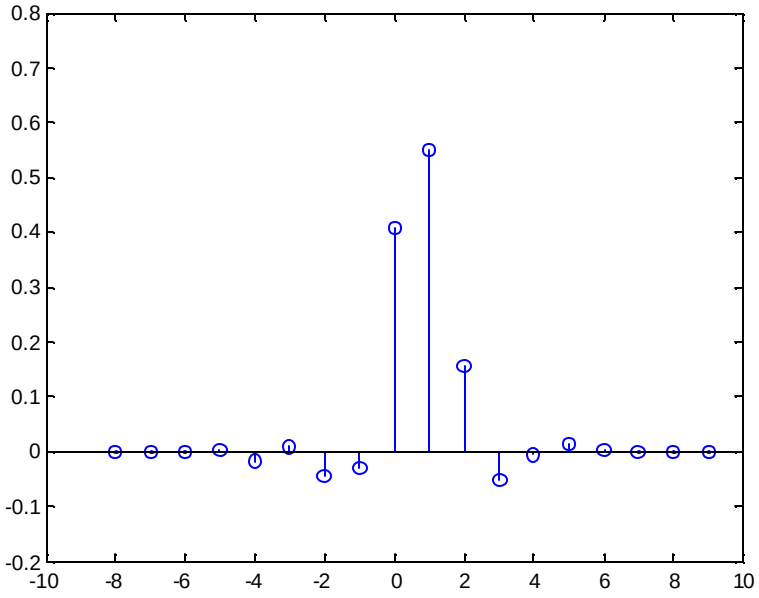

Figure 3.14:Normalized coefficients of h_0 (length= 18)

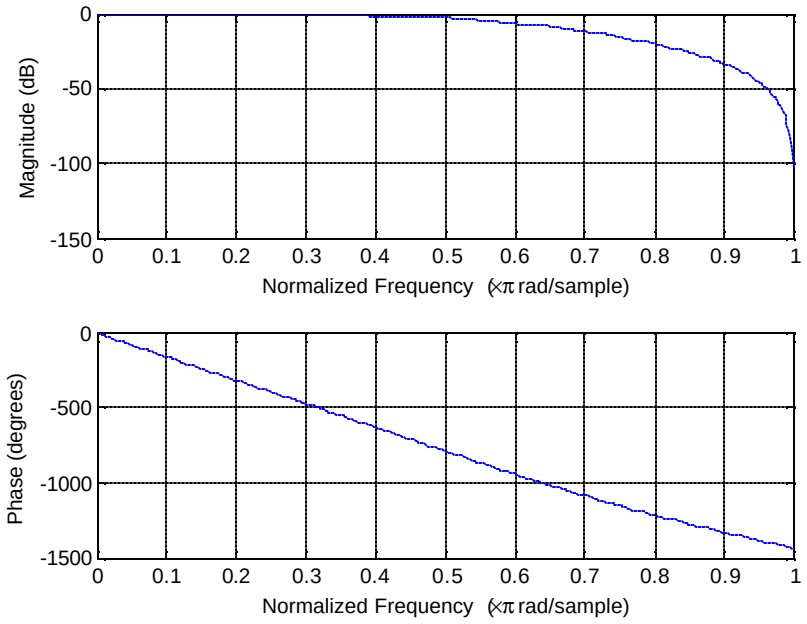

Figure 3.15: Magnitude and phase response of h_0 (length= 18)

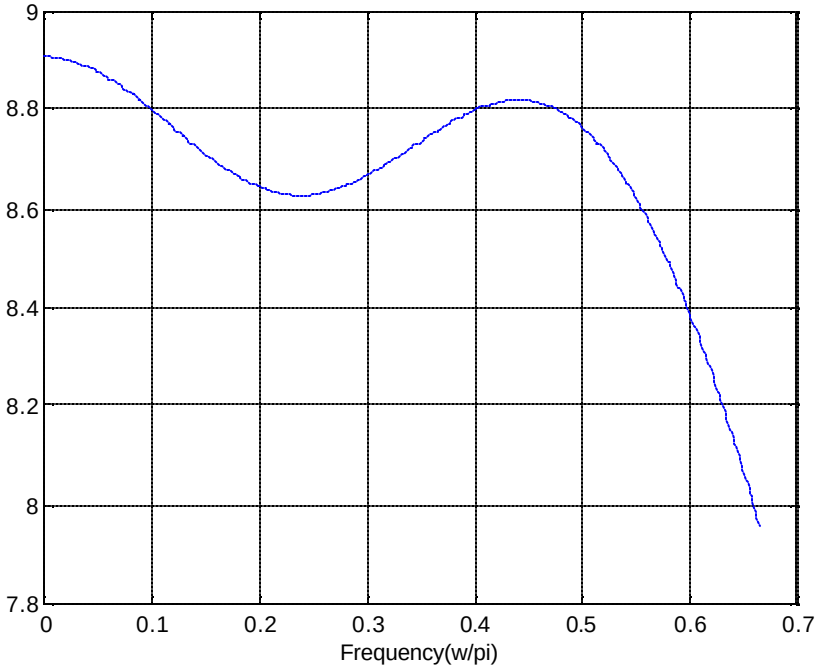

Figure 3.16: Group delay of scaling filter h_0 (length= 18)

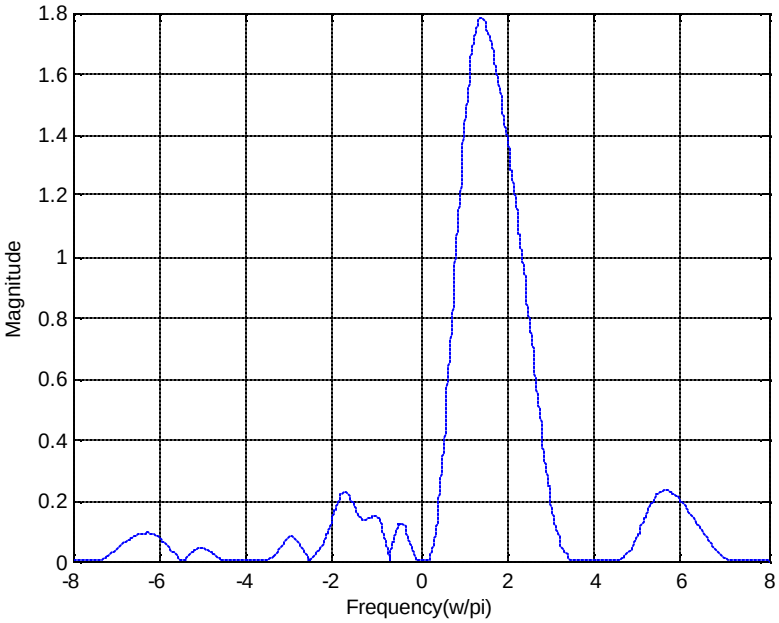

Figure 3.17: Magnitude spectra of complex wavelets $y_h + jy_g$ (length= 18)

The proposed Q-shift filter design technique is applied for different length filters. We can see vanishing moments (number of zeros at z = -1) from filter coefficients in Table 3.1, and from the figures we can conclude that our designed Q-shift filter satisfying the mentioned properties we defined before. The magnitude and phase of filters in figures shows the minimum magnitude of filter in [2p/3, p] and our filter has linear phase in [0, 2p/3). Figures 3.4, 3.8, 3.12, and 3.16 shows that our designed filters have a desired group delay of 1/4 sample period and magnitude spectra of complex wavelets show our filter are nearly analytic.

3.6 Mathematical Properties of the Q-shift Filters

In this section mathematical properties of the designed Q-shift filters are compared with Kingsbury's Q-shift filters. These mathematical features can be compared according to their moments, regularities, analyticity measurement of complex wavelet filters and the half sample delay error.

One of features of wavelets are moments, they are equal to the number of roots of scaling filter at z = -1. In Section 3.2 we talked about the vanishing moments. Both designed Q-shift filter in this work and Kingsbury's Q-shift have two vanishing moments. Vanishing moments effects on regularity, or smoothness of wavelets.

An important property of wavelet is its smoothness. Smoother wavelets provide sharper frequency resolution of functions. Holder and Sobolev regularities [17] used to characterize smoothness of wavelets. For a smooth convergence of the iterated filter bank the minimum of regularity is required [17].

By knowing the concept of complex wavelet filters in DT CWT, and according to Figure 3.1, we define complex wavelet filter as:

$$P(jw) = H_0(jw) + jG_0(jw) \tag{3. 20}$$

As we mentioned in Section 2.3.2, the complex wavelet is analytic if and only if CQFs satisfy the one sample delay in first level and the half sample delay condition in next levels [16]. This property makes wavelets form Hilbert transform pairs and the DT CWT become nearly shift invariant.

All these condition are gathered in Theorem 4 of [16] that indicates the DT CWT is μ-shift-invariant at levels more than one if and only if the CQFs satisfy the one sample delay condition in the first level and half sample delay condition in high levels, and CQFs are supported in [-2p/3, 2p/3]. The cut off frequency 2p/3 is used in designing filter for DT CWT in this work and Kingsbury's work in [9]. The support of CQFs in DT CWT is in [0, p). For the μ-shift-invariant system the magnitude spectrum (energy) of its output is insensitive to input shift, and the phase changes linearly [16]. So the energy is used to calculate the errors in sequel.

By measuring the following errors we want to know that how much our complex wavelet filter is analytic or how much the CQFs are shift invariance. The half sample delay errors show how the CQFs could make a half sample delay related to the analyticity of the complex wavelets. Smaller errors indicate better designed filters.

The analyticity measure of complex wavelet filter is obtained by

$$I_2 = \frac{\int_0^{p} |P(jw)|^2 dw}{\int_{-p}^{p} |P(jw)|^2 dw} \tag{3.21}$$

and

$$I_\infty = \frac{\max_{w\in[0,p)} |P(jw)|}{\max_{w\in[-p,p)} |P(jw)|} \quad . \tag{3.22}$$

For the CQFs, the shift invariance measure can be obtained from I_{2H} and I_{2G}

$$I_{2H} = \frac{\int_{2p/3}^{p} |H_0(jw)|^2 dw}{\int_0^{p} |H_0(jw)|^2 dw} \tag{3.23}$$

and

$$I_{2G} = \frac{\int_{2p/3}^{p} |G_0(jw)|^2 dw}{\int_0^{p} |G_0(jw)|^2 dw} \quad . \tag{3.24}$$

Other indices for measuring the shift invariance property of filters are

$$I_{\infty H} = \frac{\max_{w\in[2p/3,p)} |H_0(jw)|}{\max_{w\in[0,p)} |H_0(jw)|} \tag{3.25}$$

and

$$I_{\infty G} = \frac{\max_{w\in[2p/3,p)} |G_0(jw)|}{\max_{w\in[0,p)} |G_0(jw)|} \quad . \tag{3.26}$$

And the energy of half-sample delay error is obtained by the following formulas:

$$E_2 = \frac{\int_{-p}^{p} \left| H_0(jw) - e^{-jw} G_0(jw) \right|^2 dw}{\int_{-p}^{p} \left| H_0(jw) \right|^2 dw} \tag{3.27}$$

and

$$E_\infty = \frac{\max_{w \in [-p,p)} \left| H_0(jw) - e^{jw} G_0(jw) \right|}{\max_{w \in [-p,p)} \left| H_0(jw) \right|} \tag{3.28}$$

Results of these properties for designed filter in this work and for Kingsbury's filter for length of 12, 14, 16, and 18 (all with 2 vanishing moments) are shown in Tables 3.2 and 3.3 respectively for comparison.

Table 3.2: Mathematical properties of designed Q-shift filter

N	**Sobolev Reg.**	**Holder Reg.**	I_2	I_{2H}	I_{2G}	E_2	I_∞	$I_{\infty H}$	$I_{\infty G}$	E_∞
12	1.4887	1.0377	0.3059	0.0100	0.0100	0.0080	0.8401	0.3057	0.3057	0.1289
14	1.0409	0.7959	0.3397	0.0040	0.0040	0.0169	0.8650	0.1209	0.1209	0.1834
16	1.1295	0.8706	0.2976	0.0090	0.0090	0.0336	0.8015	0.2780	0.2780	0.2184
18	1.2811	1.0091	0.2993	0.0129	0.0129	0.0097	0.8585	0.3320	0.3320	0.1509

Table 3.3: Mathematical properties of Kingsbury's Q-shift filter

N	**Sobolev Reg.**	**Holder Reg.**	I_2	I_{2H}	I_{2G}	E_2	I_∞	$I_{\infty H}$	$I_{\infty G}$	E_∞
12	1.4410	1.0754	0.3059	0.0023	0.0023	0.0040	0.8184	0.1744	0.1744	0.0918
14	1.5300	1.3164	0.3087	0.0020	0.0020	0.0002	0.8274	0.1815	0.1815	0.0248
16	1.5694	1.3647	0.3082	0.0017	0.0017	0.00009	0.8298	0.1728	0.1728	0.0125
18	1.8292	1.5323	0.3109	0.0006	0.0006	0.0001	0.8205	0.1204	0.1204	0.0193

We also illustrate the results using diagrams. According to the results from Tables 3.2 and 3.3 or Figures 3.18 and 3.19 we see that the smoothness of designed Q-shift filter in this work is better than the smoothness of Kingsbury's Q-shift filter.

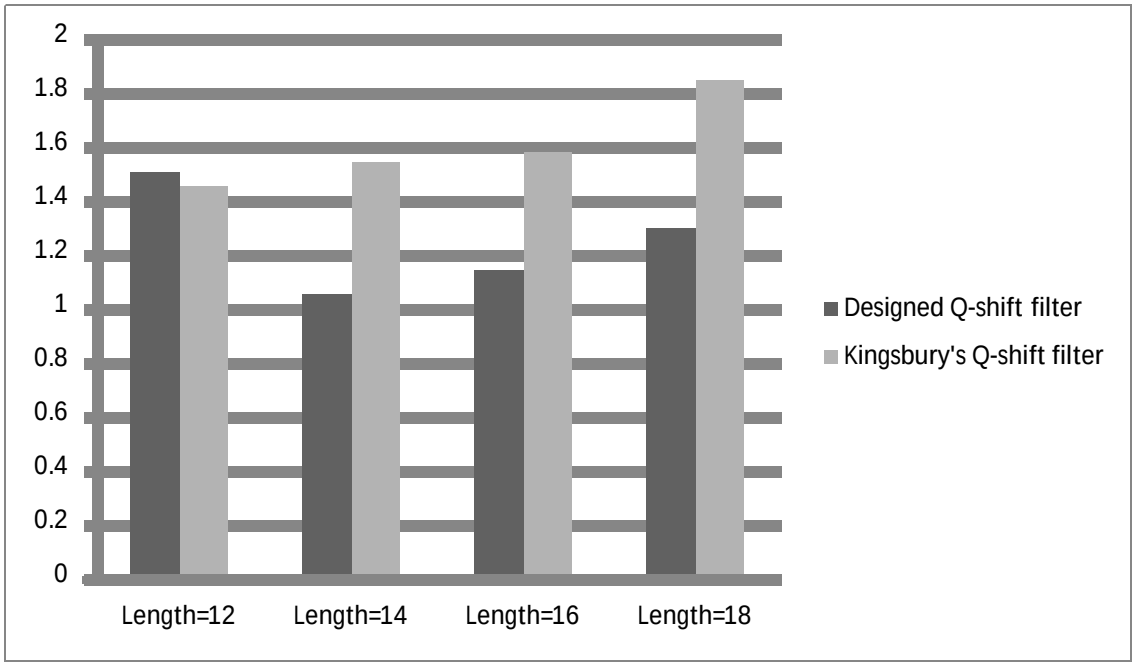

Figure 3.18: Comparison of Sobolev regularity

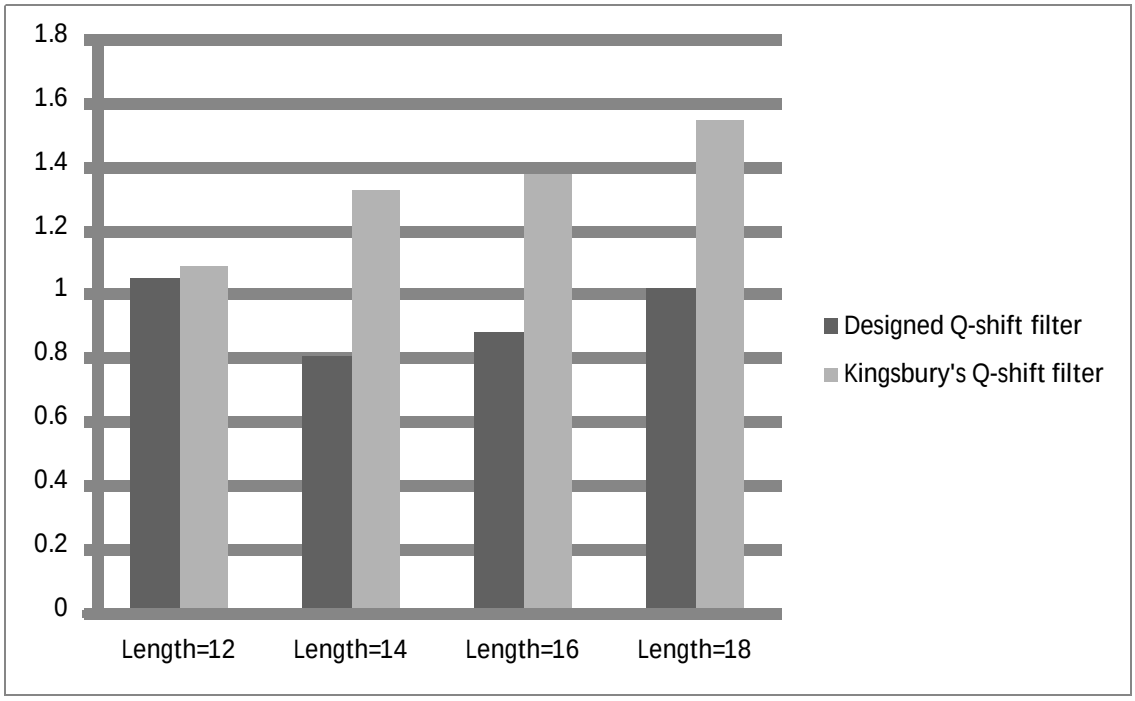

Figure 3. 19: Comparison of Holder regularity

Figures 3.20 and 3.21 illustrate the comparison of analyticity measure of complex filters for both Q-shift filters. From Table 3.2 and 3.3 and Figures 3.20 and 3.21 the analyticity measure of complex wavelet filter I_2 and I_∞ the designed Q-shift filter in this work is smaller than the analyticity measure Kingsbury's Q-shift. So the complex wavelets of designed Q-shift filter in this work are more analytic.

The comparison results of shift invariance measure are shown in Figures 3.22 and 3.23. Results of I_{2H} are similar with I_{2G} and $I_{\infty H}$ are similar with $I_{\infty G}$. We show shift invariance measure just for I_{2H} and $I_{\infty H}$.

From the tables and figures shift invariance measures of Kingsbury's Q-shift filter are smaller than the CQF's in this work. This indicates that shift invariance property of Kingsbury's Q-shift filter for CQFs is better than the designed Q-shift filter.

Figures 3.24 and 3.25 are shown the errors of half sample delay (E_2 and E_∞). According to Tables 3.2 and 3.3 and Figures 3.24 and 3.25, the half-sample delay error of Kingsbury's Q-shift filter is smaller than the half-sample delay error of the designed Q-shift filter.

The difference between errors is related to the designed procedure of both Q-shift filters. Kingsbury minimize the energy of H_{L2} and we minimize the peak magnitude of H_{L2}.

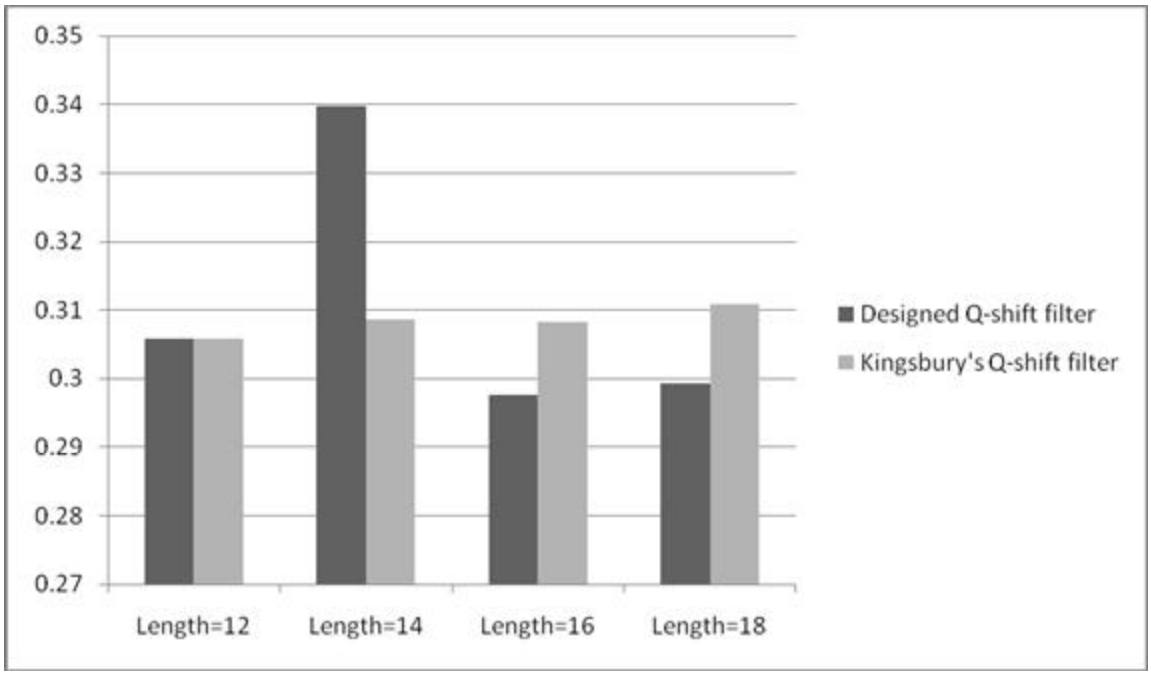

Figure 3.20: Comparison of analyticity measure (I_2)

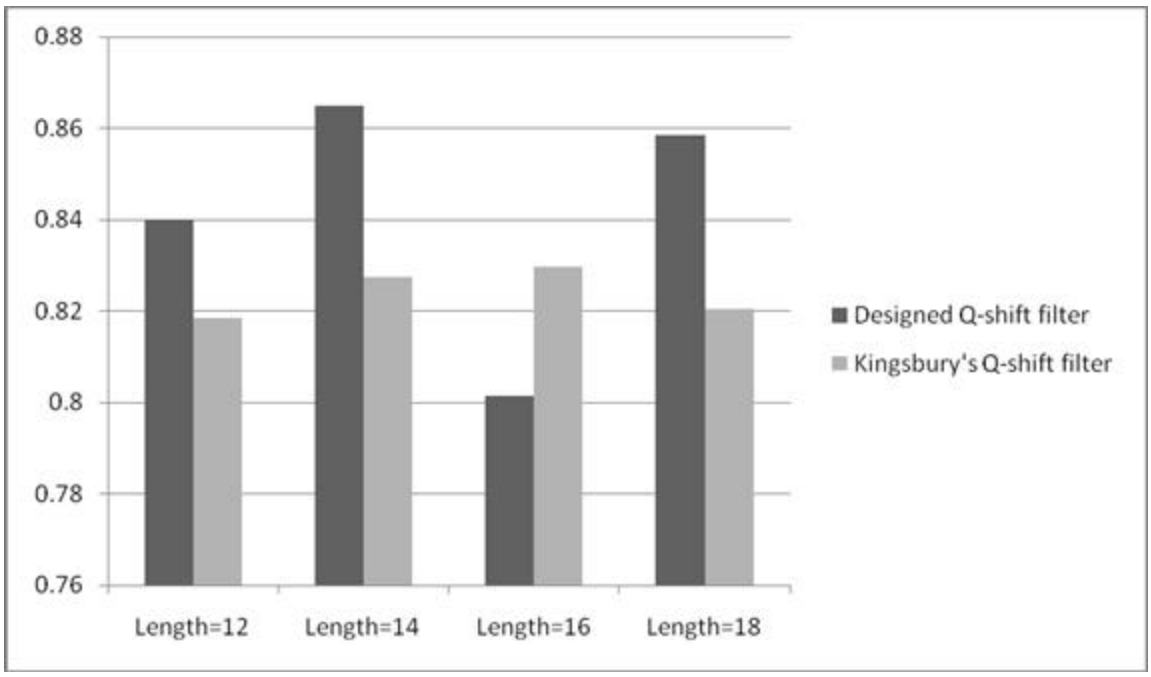

Figure 3.21: Comparison of analyticity measure (I_∞)

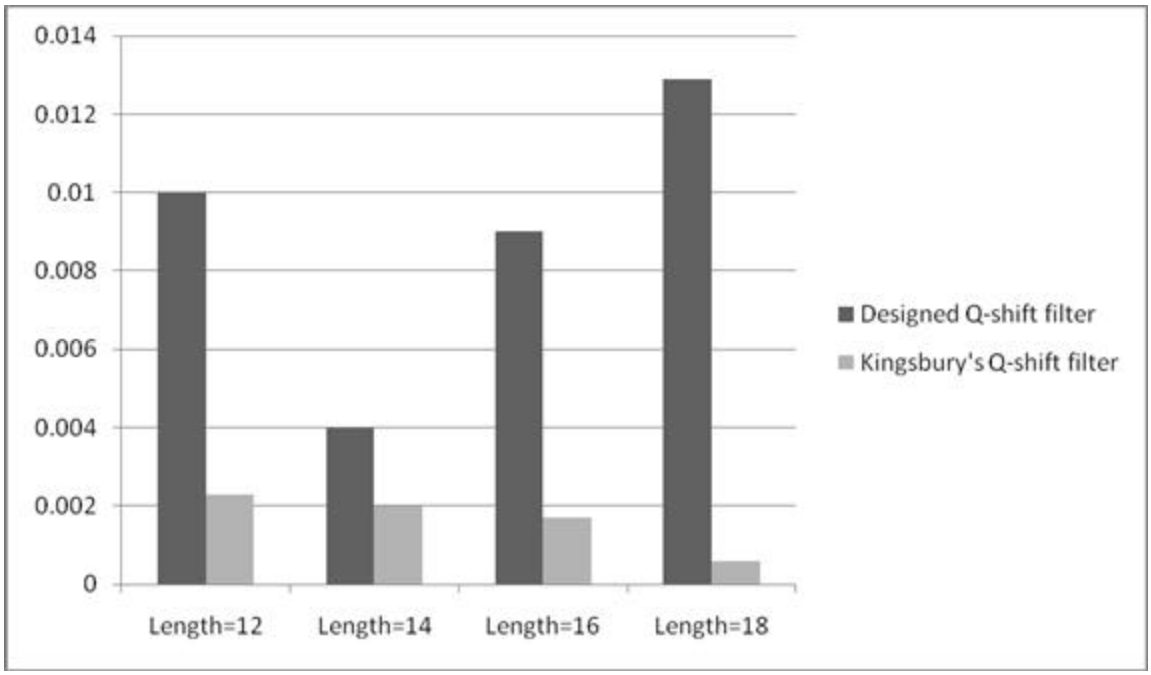

Figure 3.22: The comparison results of shift invariance measure (I_{2H})

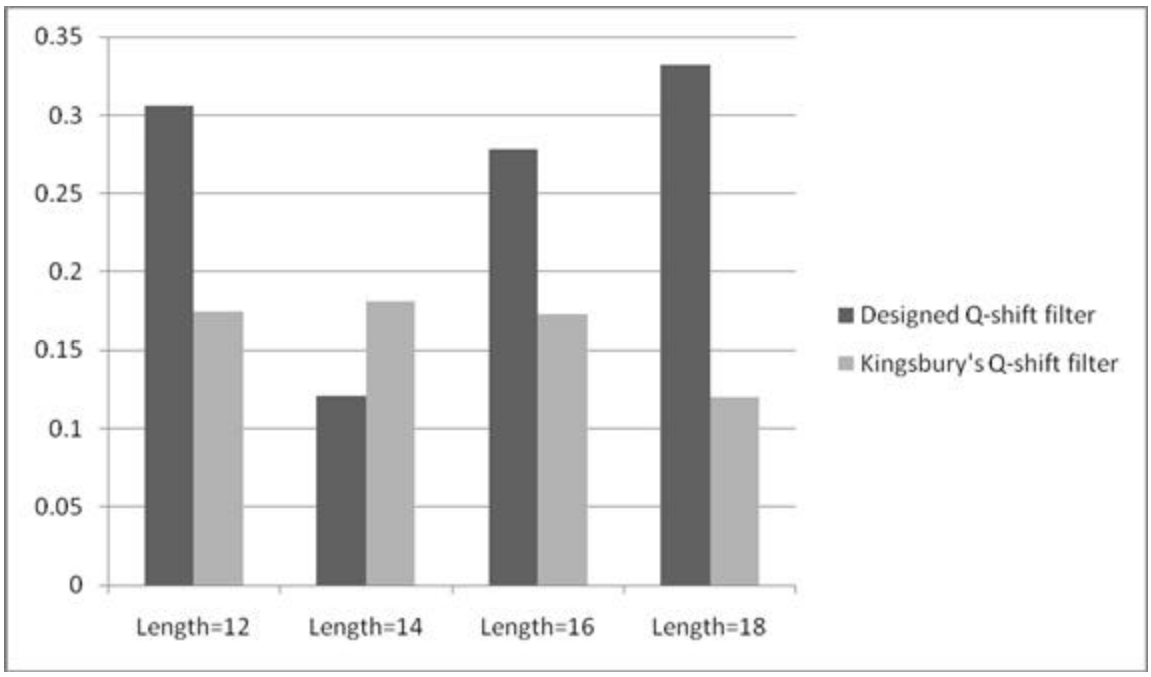

Figure 3.23: The comparison results of shift invariance measure ($I_{\infty H}$)

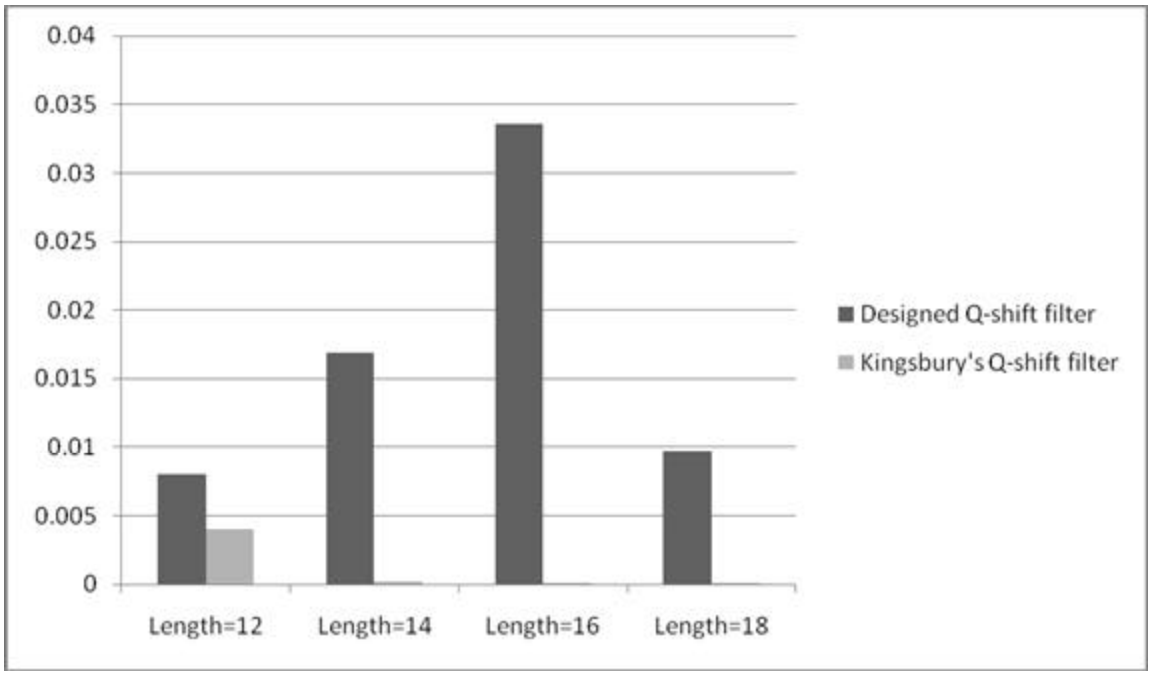

Figure 3.24: The half-sample delay error (E_2)

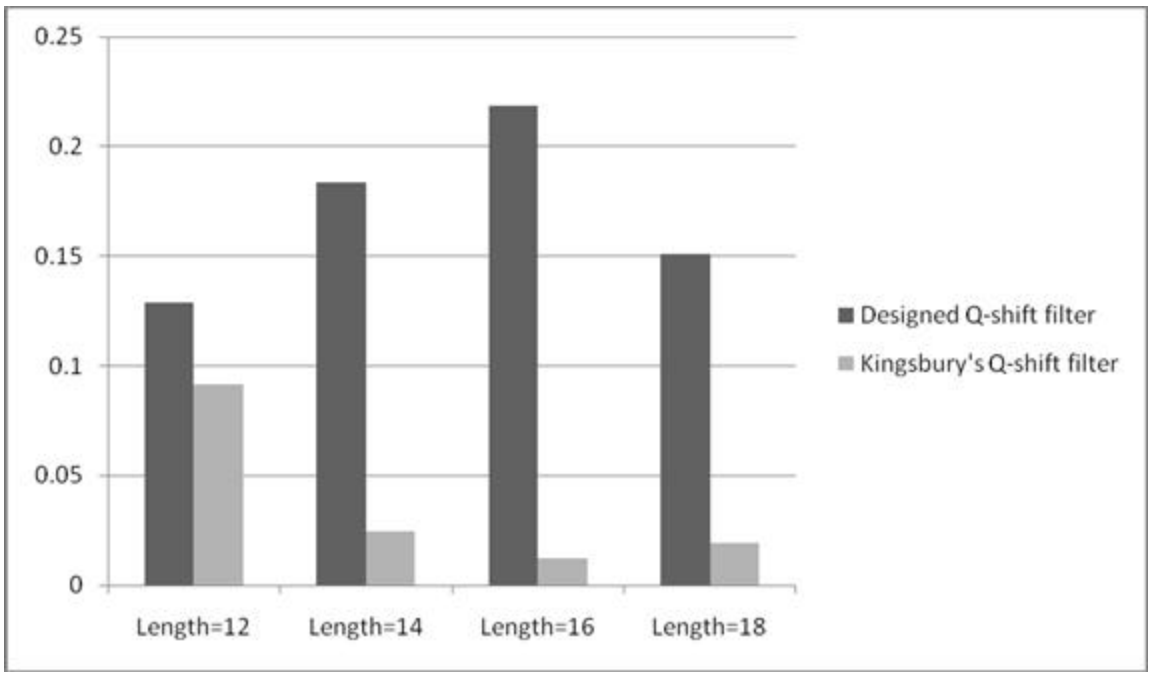

Figure 3.25: The half-sample delay error (E_∞)

Chapter 4

IMAGE DENOISING USING Q-Shift FILTERS

4.1 Introduction

The aim of this chapter is to introduce the application of our recently proposed q-shift filter bank in image denoising. We hope that the dual-tree complex wavelet transform using the Q-shift filters is advantageous in image processing applications. The application of designed Q-shift filter is shown in removing additive noise from a noisy image (denoising). Next Section shows image denoising using the designed q-shift filter.

4.2 Image Denoising Using the Designed Q-shift Filter

One technique for denoising is wavelet thresholding or shrinkage. In recent years there have been many studies on using wavelet thresholding for denoising in signal processing. Two methods for denoising have been proposed: linear and nonlinear. Thresholding belongs to the nonlinear category. It gives a simple denoising scheme by applying to wavelet coefficients [18]. As we know, all details in image are in high frequency sub-bands, the idea of thresholding is to set all high frequency sub-band coefficients that are less than a particular threshold to zero. These coefficients are used in an inverse wavelet transformation to reconstruct the data set. The wavelet transform yields a large number of small coefficients and a small number of large coefficients. In simple denoising using wavelet transform, the wavelet transform of noisy signal is

calculated, the noisy wavelet coefficients according to some role are modified and the inverse transform according the modified coefficients computed. The mentioned methods use a threshold value that must be estimated correctly in order to obtain good performance.

The employed denoising technique is based on Bivariate Shrinkage [19, 20], that will be explained in next section.

4.2.1 Bivariate Shrinkage Denoising

This technique is based on the modeling of the wavelet transform coefficients of natural images. The denoising of natural images corrupted by Gaussian noise is a classical problem in signal processing. The wavelet transform has become an important tool for this problem due to its energy compaction property.

A new simple non-Gaussian bivariate probability distribution function has been proposed by Sendur and Selesnick [19, 20] to model the statistics of wavelet coefficients of natural images. In this work the denoising of an image corrupted by white Gaussian noise will be considered.

The problem is formulated as

$$g = x + n \tag{4.1}$$

where g is noisy signal and x is the desired signal that should be estimated according to some criteria where n is independent Gaussian noise. In wavelet domain, the problem can be reformulated as

$$y = w + n \tag{4.2}$$

where $y = (y_1, y_2)$ is noisy wavelet coefficients, $n = (n_1, n_2)$ is noise coefficients, which is independent Gaussian, and $w = (w_1, w_2)$ is true wavelet coefficients. Let w_2 be the

parent wavelet coefficient of w_1 at the same spatial position with different scale. n_1 and n_2 are identically and independently distributed Gaussian noise with the same variance s_n^2. The following non-Gaussian bivariate shrinkage probability distribution function (pdf) is used in bivariate shrinkage denoising algorithm:

$$p_w(w) = \frac{3}{2p\,s^2} e^{-\frac{\sqrt{3}}{s}\sqrt{w_1^2+w_2^2}} \quad . \tag{4.3}$$

With this pdf, w_1 and w_2 are uncorrelated, but not dependent; s^2 is the signal variance for each wavelet coefficient. The maximum a posteriori estimator (MAP) of w_1 yields the following bivariate shrinkage function:

$$\hat{w}_1 = \frac{y_1}{\sqrt{y_1^2 + y_2^2}} \max\left\{\sqrt{y_1^2 + y_2^2} - \frac{\sqrt{3}s_n^2}{s}, 0\right\} \quad . \tag{4.4}$$

From [21] for this bivariate function, the greater values for the shrinkage are obtained when the smaller values are chosen for the parent. For this shrinkage function both signal variance and noise variance should be known for each wavelet coefficient and at first these parameters are estimated by algorithm.

To summarize, the algorithm has two steps: at first the noise variance is calculated, then for each wavelet coefficient signal variance is calculated. Each coefficient is estimated by using the bivariate shrinkage function.

4.3 Experimental Results

We used three standard images (Boat, Baboon, and Cameraman) of size 512×512 for test. Each image is corrupted by an additive white Gaussian noise at different noise levels and then denoised using the bivariate shrinkage algorithm [19]. In our experiment we use two DT filter banks. The first one is Kingsbury's q-shift

orthogonal solution of length 14/14 [9], the other one is our designed q-shift of length 14/14. As mentioned before, different filter banks are used in the first stage of implementation of the transform. We use the Daubechies 9/7 filters in the first stage in both designs. The performance is evaluated by the peak signal-to-noise ratio (in decibel) using $PSNR = 20\log_{10}(25/e_{rms})$ with e_{rms} being root mean square error between the noisy and original image. The numerical results of PSNR are tabulated in Table 4.1. Results using other filters designed for DT CWT can be found in [18].

We present the original, noisy and typical denoised images of three test images in Figures 4.1, 4.2, 4.3. Denoising results in these figures show that Kingsbury's Q-shift filter's performance is better than the Q-shift filter designed in this work.

As mentioned in Section 3.6 the difference between the results of both designed Q-shift filters are related to the method that has been used for magnitude minimization of H_{L2} in designing procedure. Kingsbury's method of minimization is on the energy of H_{L2} whereas we minimize the peak magnitude of H_{L2}. This difference may be the reason for better PSNR results of Kingsbury's Q-shift filters.

Table 4.1: Averaged PSNR values (in dB) of denoised images for different noisy images

Images	Noisy Image	Designed Q-shift Filter	Kingsbury's Q-shift Filter
Boat			
$s = 10$	13.63	33.49	34.34
$s = 15$	13.45	31.08	32.21
$s = 20$	13.20	29.33	30.74
$s = 25$	12.90	27.87	29.69
$s = 30$	12.56	26.77	28.81
Baboon			
$s = 10$	15.38	28.76	29.51
$s = 15$	15.09	26.61	27.59
$s = 20$	14.73	25.07	26.18
$s = 25$	14.31	23.77	25.14
$s = 30$	13.83	22.79	24.27
Cameraman			
$s = 10$	12.21	35.19	36.53
$s = 15$	12.07	32.66	34.34
$s = 20$	11.88	30.99	32.89
$s = 25$	11.65	29.68	31.74
$s = 30$	11.40	28.70	30.85

(a)

(b)

(c)

(d)

Figure 4.1: Boat: (a) Original image, (b) Noisy image ($s = 10$, PSNR= 13.6335), (c) Denoised image by Kingsbury's Q-shift filter (PSNR= 34.3487), (d) Denoised image by designed Q-shift filter (PSNR= 33.4932)

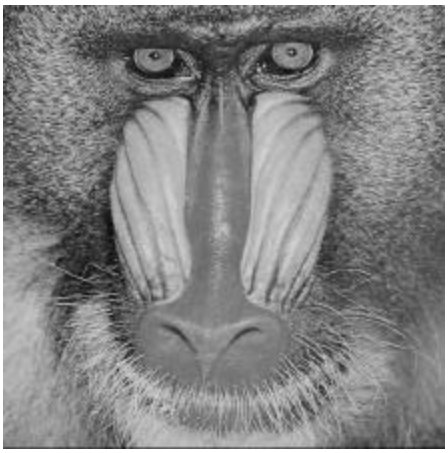

(a)

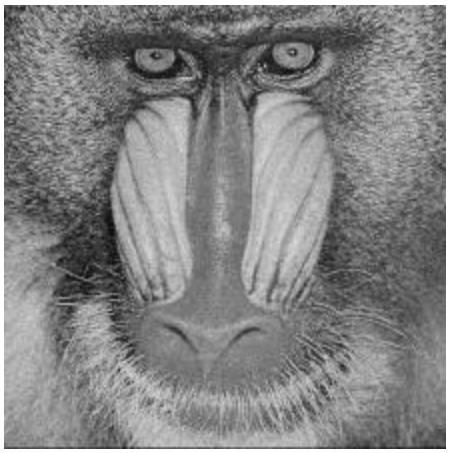

(b)

(c)

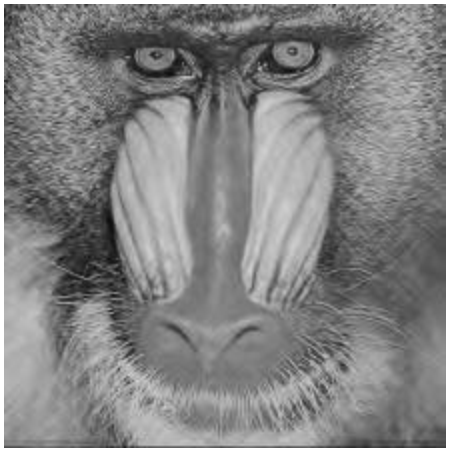

(d)

Figure 4.2: Baboon (a) Original image, (b) Noisy image ($s = 15$, PSNR= 15.0952), (c) Denoised image by Kingsbury's Q-shift filter (PSNR= 27.5924), (d) Denoised image by designed Q-shift filter (PSNR= 26.6104)

(a)

(b)

(c)

(d)

Figure 4.3: Cameraman (a) Original image, (b) Noisy image ($s = 25$, PSNR= 11.6575), (c) Denoised image by Kingsbury's Q-shift filter (PSNR= 31.7490), (d) Denoised image by designed Q-shift filter (PSNR= 29.6833)

Chapter 5

CONCLUSION AND FUTURE WORK

This work is concerned with the design of filter for DT CWT structure. Introducing the DT CWT structure and its properties that provide shift invariance and directional selectivity of filter banks with a limit redundancy a new design of Q-shift filters is presented. The Q-shift filter is motivated by Kingsbury's work for improving orthogonality and symmetry properties. In this work we complemented Kingsbury's approach with a new method of designing.

Considering the requirements of Q-shift filters such as no aliasing, perfect reconstruction, orthogonality, group delay of 1/4 sample, good smoothness and finite support in (-2p/3, 2p/3), a new design of Q-shift filter via parameterization method is proposed. With this method the space of orthonormal filter banks is parameterized and the parameters are used in designing filter with desirable properties. The constraints that have been used in this method guaranteed two vanishing moments of wavelets.

In designing of both Q-shift filters for obtaining the group delay of 1/4 and 3/4 samples the 4L tap, linear phase and symmetric low pass filter (H_{L2}) have been used.

For obtaining the desirable property of 1/4 and 3/4 sample period we minimized the peak magnitude of H_{L2} in [p/3, p] instead of minimizing energy used by Kingsbury [9].

Results of designing are shown that the desirable mentioned properties are obtained for the Q-shift filter. The designed Q-shift filter is compared with Kingsbury's Q-shift approach according to analyticity measurement, shift invariance and half-sample delay, which are the most important properties of wavelet filters in dual-tree filter banks.

The designed Q-shift filter is applied in image denoising. Three standard image that corrupted by an additive Gaussian noise are used. The Bivariate shrinkage algorithm is employed for wavelet coefficient modeling and thresholding. The performance (PSNR) of Kingsbury's Q-shift filter (L= 14) is better than that of the designed filter (L= 14) in this work. Both filters have the same performance in visual.

The difference between results related the optimization method that has been used in this method. Kingsbury minimized the energy of H_{L2} in the [p/3, p] and we minimized the peak magnitude of H_{L2} in this work.

The most important reason of using the mentioned method of designing Q-shift filter in this work is that the method has perfect orthogonality whereas Kingsbury's approach is approximate. It guarantees two vanishing moments by using simple constraints and using a simple method of optimization.

As a future work we can explore other image applications where the designed filters may be of advantages due to the small peak error property.

REFERENCES

[1] N. G. Kingsbury, ''The dual-tree complex wavelet transform: A new technique for shift invariance and directional filters,'' in Proceeding of the 8th IEEE DSP Workshop, Utah, paper no. 86, 9-12 Aug 1998.

[2] I. W. Selesnick, R. G. Baruniuk, and N. G. Kingsbury, ''The Dual-tree complex transform- a coherent framework for multiscale signal and image processing.'' IEEE Signal Processing Mag., vol.6, pp. 123-151, Nov 2005.

[3] I. W. Selesnick, ''Hilbert transform pairs of wavelet bases'', IEEE Signal Processing Letters, vol. 8, no. 6, pp.170-173, Jun 2001.

[4] R. Yu and H. Ozkaramanli, ''Hilbert transform pairs of orthogonal wavelet bases: Necessary and sufficient conditions'', IEEE Trans. on Signal Processing, vol. 53, no. 12, pp. 4723-4725, Dec 2005.

[5] M. Antonini, M. Barlaud, P. Mathieu and I. Daubechies, ''Imaging coding using wavelet transform'', IEEE Trans. on Image Processing, vol. 1, pp. 205-220, Apr. 1992.

[6] I. W. Selesnick, ''The Design of approximate Hilbert transform pairs of wavelet bases'', IEEE Trans. on Signal Processing, vol. 50, no.5, pp. 1144-1152, May 2002.

[7] N. G. Kingsbury, ''The dual-tree complex wavelet transform with improved orthogonality and symmetry properties'', in Proc. IEEE Int. Conf. Image Processing, Vancouver, BC, Canada, vol. 2, pp. 375-378, 10-13 Sep 2000.

[8] N. G. Kingsbury, ''Complex wavelets for shift invariance analysis and filtering of signals'', Applied and Computational Harmonic Analysis, vol. 10, no. 3, pp. 234-253, May 2001.

[9] N. G. Kingsbury, ''Design of q-shift complex wavelets for image processing using frequency domain energy minimization'', In Proc. of IEEE Int. Conf. Image Processing, Barcelona, vol. 1, pp. 1013-1016, Sep 2003.

[10] B. G. Sherlock and D. M. Monro, ''On the space of orthonormal wavelets'', IEEE Trans. Signal Process, vol. 46, no. 6, pp. 1716-1720, Jun 1998.

[11] H. M. Paiva, M. N. Martins, R. K. Galvao and J. P. M. Paiva, ''On the space of orthonormal wavelets: Additional constraints to ensure two vanishing moments'', IEEE Signal Processing Letters, vol. 16, no. 2, pp. 101-104, Feb 2009.

[12] C. Sidney Burrus, R.A Gopinath and Haitao Guo, ''Introduction to Wavelets and Wavelet Transforms'' Prentice Hall, New Jersy, 1998.

[13] R. Yu and A. Baradarani, ''Sampled-data design of FIR dual filter banks for dual-tree complex wavelet transform'', IEEE Trans. on Signal Processing, vol. 56, pp. 3369-3375, Jun 2008.

[14] R. Yu, ''Characterization and sampled-data design of dual-tree filter banks for Hilbert transform pairs of wavelet bases'', IEEE Trans. on Signal Processing, vol. 55, pp. 2458-2471, Jun 2007.

[15] N. G. Kingsbury, ''Dual Tree Complex Wavelets'', HASSIP Workshop, Cambridge, Sep 2004.

[16] R. Yu, ''A new shift-invariance of discrete –time systems and its application to discrete wavelet transform analysis'', IEEE Trans. on Signal Processing., vol. 57, no. 7, July 2009.

[17] M. Unser and T. Blue, ''Mathematical properties of the JPEG2000 wavelet filters'', IEEE Trans. on Image Processing, vol. 12, pp. 1080-1090, Sep 2003.

[18] A. Baradarani and R. Yu, ''A dual-tree complex wavelet with application in image denoising'', in Proceeding of the IEEE Int. conf. on Signal Processing and Communication, Dubai, UAE, pp. 1203-1206, Nov 2007.

[19] L. Sendur and I. W. Selesnick, ''Bivariate shrinkage with local variance estimation'', IEEE Signal Processing Letters, vol. 9, pp. 438-441, Dec 2002.

[20] L. Sendur and I. W. Selesnick, ''Bivariate shrinkage functions for wavelet-based denoising exploiting inter scale dependency'', IEEE Trans. on Signal Processing, vol. 50, pp. 2744-2756, Nov 2002.

[21] I. W. Selesnick, Matlab Implementation of Wavelet Transforms, http://taco.poly.edu/WaveletSoftware/